MPP-2012-104

arXiv:1208.2951v1 [hep-ph] 14 Aug 2012

Axions and saxions from the primordial supersymmetric plasma and extra radiation signatures

Peter Graf and Frank Daniel Steffen
Max-Planck-Institut für Physik, Föhringer Ring 6, D–80805 Munich, Germany

We calculate the rate for thermal production of axions and saxions via scattering of quarks, gluons, squarks, and gluinos in the primordial supersymmetric plasma. Systematic field theoretical methods such as hard thermal loop resummation are applied to obtain a finite result in a gauge-invariant way that is consistent to leading order in the strong gauge coupling. We calculate the thermally produced yield and the decoupling temperature for both axions and saxions. For the generic case in which saxion decays into axions are possible, the emitted axions can constitute extra radiation already prior to big bang nucleosynthesis and well thereafter. We update associated limits imposed by recent studies of the primordial helium-4 abundance and by precision cosmology of the cosmic microwave background and large scale structure. We show that the trend towards extra radiation seen in those studies can be explained by late decays of thermal saxions into axions and that upcoming Planck results will probe supersymmetric axion models with unprecedented sensitivity.

PACS numbers: 14.80.Va, 11.30.Pb, 98.80.Cq, 98.80.Es

I. INTRODUCTION

There are several hints towards physics beyond the standard model (SM). One of them is the strong CP problem. If this problem is solved via the Peccei–Quinn (PQ) mechanism, the axion a arises as the pseudo-Nambu-Goldstone boson associated with the $\mathrm{U}(1)_{\mathrm{PQ}}$ symmetry broken spontaneously at the PQ scale f_{PQ} [1, 2]. Another attractive extension of the SM is supersymmetry (SUSY) [3–6]. In conceivable settings with both the PQ mechanism and SUSY, the pseudo-scalar axion is part of a supermultiplet in which also its scalar partner, the saxion σ, and its fermionic partner, the axino $\tilde{a}$, appear. The energy density of the early Universe can then receive contributions from coherent oscillations of the axion field [1, 2, 7] and the saxion field [8–12] and from thermal production of axions [1, 13–17], saxions [8, 10, 18], and axinos [19–29] in the hot primordial plasma.

Here we calculate for the first time the thermal production rate of axions and saxions via scattering processes of quarks, gluons, squarks, and gluinos in a gauge-invariant way consistent to leading order in the strong coupling constant g_s. In our calculation we use hard thermal loop (HTL) resummation [30] and the Braaten–Yuan prescription [31] to account systematically for screening effects in the quark-gluon-squark-gluino plasma (QGSGP). This method was introduced on the example of axion production in a hot QED plasma [31]; see also Ref. [32]. Moreover, it has been applied to calculate the thermal production of gravitinos [32–35] and axinos [24] in SUSY settings and of axions in a non-SUSY quark-gluon plasma (QGP) [17, 36].

Based on our result for the thermal axion/saxion production rate, we determine the respective thermally produced yields and estimate the decoupling temperature of axions and saxions from the thermal bath. While both axions and axinos are promising dark matter candidates (cf. [1, 2, 37, 38] and references therein), saxions can be late decaying particles with potentially severe cosmological implications. For example, energetic hadrons and photons from saxion decays during or after big bang nucleosynthesis (BBN) can change the abundances of the primordial light elements [11]. Moreover, photons from saxion decays can affect the black body spectrum of the cosmic microwave background (CMB) for a saxion lifetime of $10^6\,\mathrm{s} \lesssim \tau_\sigma \lesssim 10^{13}\,\mathrm{s}$ [11, 39] or may contribute either to the diffuse $X(\gamma)$-ray background or as an additional source of reionization for $\tau_\sigma \gtrsim 10^{13}\,\mathrm{s}$ [11, 39–41]. In scenarios in which the decay mode into axions is not the dominant one, saxion decays may also produce significant amounts of entropy [9, 18, 39, 42–44]. This can dilute relic densities of species decoupled from the plasma and also the baryon asymmetry η. Then, $\tau_\sigma < 1$ s is imposed by successful BBN which requires a standard thermal history for temperatures below $T \sim 1$ MeV.

In this work, however, we look at scenarios in which saxions (from thermal processes) decay predominantly into axions. Moreover, we still focus on decays prior to BBN and compute the additional radiation provided in the form of the emitted relativistic axions. Such a non-standard contribution ΔN_{eff} to the effective number of light neutrino species N_{eff} from decays of thermal saxions into axions was previously considered in Refs. [8, 11, 21, 45]. Applying our new result for the thermally produced saxion yield and new cosmological constraints on ΔN_{eff} imposed by recent studies of BBN, the CMB, and large scale structure (LSS) [46–48], we present updated limits on the PQ scale f_{PQ}, the saxion mass m_σ, and the reheating temperature T_{R} after inflation.

Interestingly, precision cosmology [48–52] and recent studies of the primordial ^{4}He abundance [46, 47] show a trend towards a radiation content that exceeds the predictions of the SM. In fact, such an excess can be explained by the considered saxion decays into axions. The observed trend may thus be a hint for the existence of a SUSY axion model. Here results from the Planck satellite mission will be extremely valuable, which will come with an unprecedented sensitivity to the amount of extra radiation at times much later than those at which BBN probes this quantity. Based on a forecasted 68% confidence level (CL) sensitivity of $\Delta N_{\rm eff} = 0.26$ [53, 54], we indicate parameter regions of SUSY axion models that will be tested by results from the Planck satellite mission expected to be published in the near future.

The remainder of this paper is organized as follows. In the next section we consider interactions of the PQ supermultiplet and decay widths for saxion decays. In Sects. III and IV our calculations of the thermal production rates of saxions and axions are presented. We compute the associated yields in Sect. V and use the results to estimate the saxion/axion decoupling temperature in Sect. VI. Then we explore $\Delta N_{\rm eff}$ provided in the form of axions from saxion decays and possible manifestations in studies of BBN and of the CMB and LSS. Here we comment on potential restrictions which can emerge from overly efficient thermal gravitino/axino production and describe exemplary settings that allow for a high reheating temperature of $T_{\rm R} \sim 10^8$–$10^{10}\,$GeV. In Sect. VIII we compare the relic density of axions from the misalignment mechanism with the ones of thermal axions and of non-thermal axions from saxion decays. Our conclusions are given in Sect. IX.

II. PARTICLE PHYSICS SETTING

In a SUSY framework, the $\mathrm{U}(1)_{\rm PQ}$ symmetry is extended to a symmetry of the (holomorphic) superpotential and thereby to its complex form $\mathrm{U}(1)^{\rm c}_{\rm PQ}$ [55]. In the case of unbroken SUSY, this implies the existence of a flat direction and thereby a massless saxion field. Once SUSY is broken, this flat direction gets lifted, resulting in a model-dependent mass of the saxion m_σ. For example, m_σ is expected to be of the order of the gravitino mass $m_{3/2}$ in gravity-mediated SUSY breaking models [10, 18, 39]. Here we do not look at a specific model but treat m_σ as a free parameter.

In this work we consider the particle content of the minimal supersymmetric SM (MSSM) extended by the PQ superfield $A = (\sigma + ia)/\sqrt{2} + \sqrt{2}\theta\tilde{a} + F_A\theta\theta$, where θ denotes the corresponding fermionic superspace coordinate and F_A the chiral auxiliary field. The interactions of A with the color-field-strength superfield $W^b = \tilde{g}^b + D^b\theta - \sigma^{\mu\nu}\theta G^b_{\mu\nu} + i\theta\theta\sigma^\mu D_\mu \bar{\tilde{g}}^b$ are given by the effective Lagrangian

$$\mathcal{L}^{\rm int}_{\rm PQ} = -\frac{\sqrt{2}\alpha_s}{8\pi f_{\rm PQ}} \int d^2\theta A\, W^b W^b + \text{h.c.}\ , \qquad (1)$$

where b is a color index, $\tilde{g}^b$ the gluino field, D^b the real color-gauge auxiliary field, $G^b_{\mu\nu}$ the gluon-field-strength tensor, D_μ the corresponding color-gauge covariant derivative, and $\alpha_s = g_s^2/(4\pi)$. After performing the integration, we get for the propagating fields in 4-component spinor notation:

$$\begin{aligned}\mathcal{L}^{\rm int}_{\rm PQ} =& \frac{\alpha_s}{8\pi f_{\rm PQ}}\Big[\sigma\left(G^{b\,\mu\nu}G^b_{\mu\nu} - 2D^bD^b - 2i\bar{\tilde{g}}^b_M\gamma^\mu D_\mu \tilde{g}^b_M\right) \\ &+ a\left(G^{b\,\mu\nu}\widetilde{G}^b_{\mu\nu} + 2\bar{\tilde{g}}^b_M\gamma^\mu\gamma^5 D_\mu\tilde{g}^b_M\right) \\ &- i\bar{\tilde{a}}_M\frac{[\gamma^\mu,\gamma^\nu]}{2}\gamma^5\tilde{g}^b_M G^b_{\mu\nu} + 2\bar{\tilde{a}}_M D^b\tilde{g}^b_M\Big]\ , \qquad (2)\end{aligned}$$

where $\widetilde{G}^b_{\mu\nu} = \epsilon_{\mu\nu\rho\sigma}G^{b\,\rho\sigma}/2$ and $D^b = -g_s\sum_{\tilde{q}}\tilde{q}^*_i T^b_{ij}\tilde{q}_j$ with a sum over all squark fields $\tilde{q}$ and the $\mathrm{SU}(3)_c$ generators T^b_{ij} in their fundamental representation; the subscript M indicates 4-component Majorana spinors. Note that we use the space-time metric $g_{\mu\nu} = g^{\mu\nu} = \mathrm{diag}(+1,-1,-1,-1)$ and other conventions and notations of Ref. [6] and – except for a different sign of the Levi-Civita tensor $\epsilon^{0123} = +1$ – of Ref. [4]. For comparisons with similar $\mathcal{L}^{\rm int}_{\rm PQ}$ expressions given in Refs. [25, 28], we remark that the second term in the brackets in the second line of (2) can be written as $D_\mu(\bar{\tilde{g}}^b_M\gamma^\mu\gamma^5\tilde{g}^b_M)$. However, our result for the saxion-gluino-interaction term differs from the corresponding terms in [25] and [28] by factors of -2 and -1, respectively. Moreover, our findings for the axino interactions differ by a factor of -1 from the ones in [25, 28]. This may result partially from metric conventions: If we translate (2) into the corresponding expression valid for $g_{\mu\nu} = g^{\mu\nu} = \mathrm{diag}(-1,+1,+1,+1)$ using Appendix A of Ref. [6], the sign of our result for the axino-gluino-gluon-interaction term will change, whereas all other terms in (2) will not be affected.

In the following we focus on hadronic or KSVZ axion models [56, 57] in a SUSY setting in which the effective Lagrangian (2) describes the relevant interactions even in a conceivable very hot early stage of the primordial plasma with temperatures T not too far below $f_{\rm PQ}$. Note that we do not consider scenarios with a radiation-dominated epoch with T above the masses of the heavy KSVZ (s)quarks $m_{Q,\tilde{Q}}$ such as those considered in Ref. [27].

Next we address interactions between axions and saxions in models with N SM-gauge singlet PQ multiplets Φ_i with PQ charges q_i and vacuum expectation values (VEVs) v_i after PQ symmetry breaking. Near the VEVs (after integrating out the heavy fields in the PQ sector), the scalar parts of Φ_i can be parametrized as

$$\phi_i = v_i \exp\left[\frac{q_i(\sigma + ia)}{\sqrt{2}v_{\rm PQ}}\right]\ . \qquad (3)$$

Here the canonical PQ charge normalization requires $q_i^2 = 1$ for the smallest q_i and $v_{\rm PQ} = \sqrt{\sum_i v_i^2 q_i^2}$ results from the requirement of canonically normalized kinetic terms for the axion and the saxion. Moreover, from the kinetic terms of the PQ fields, one finds that interactions between axions and saxions can emerge as follows [21]

$$\mathcal{L}^{\rm kin}_{\rm PQ} = \sum_{i=1}^{N} \partial^\mu \phi_i \partial_\mu \phi_i^* \\ \sim \left(1 + \frac{\sqrt{2}x}{v_{\rm PQ}}\sigma\right) \left[\frac{1}{2}(\partial_\mu a)^2 + \frac{1}{2}(\partial_\mu \sigma)^2\right] + \ldots \quad (4)$$

where $x = \sum_i q_i^3 v_i^2/v_{\rm PQ}^2$. The strength of these interactions thus depends on the model. For example, $x = (v_1^2 - v_2^2)/v_{\rm PQ}^2$ in models whose superpotentials contain the term $\kappa R(\Phi_1\Phi_2 - v_{\rm PQ}^2/2)$ with a Yukawa coupling κ, two PQ fields with $q_1 = -q_2 = 1$ and a SM-gauge singlet field R with $q_R = 0$. This illustrates that $x \ll 1$ is possible if $v_1 \simeq v_2 \simeq v_{\rm PQ}/\sqrt{2}$ [11, 21, 58]. On the other hand, in a KSVZ axion model with just one PQ scalar (with $v = v_{\rm PQ}$ and $q = 1$) [10], one finds $x = 1$, which is the value that we will consider in Sect. VII below.

Let us now relate the scale $v_{\rm PQ}$, imposed by canonically normalized kinetic terms, to $f_{\rm PQ}$, defined by the form of the prefactor of the effective axion-gluon interactions in (2). In a KSVZ model, those interactions emerge from axion couplings to the heavy KSVZ quarks which are described by contributions to the superpotential of the form $h\Phi_1 Q_L \bar{Q}_R$ with a Yukawa coupling h, $q_1 = 1$ and heavy quark multiplets Q_L and $\bar{Q}_R$ with color charge and PQ charges $q_Q = -1/2$. Considering the resulting Lagrangian that describes the interactions of ϕ_1 with the KSVZ quarks, one sees that the spontaneous breaking of the PQ symmetry results in heavy Dirac KSVZ quarks with a mass $m_Q = hv_1$. Integrating out loops of such heavy quarks, one finds the effective Lagrangian describing axion interactions with gluons

$$\mathcal{L}^{\rm int} = \frac{hv_1\alpha_s}{8\pi\sqrt{2}\, m_Q v_{\rm PQ}}\, a\, G^{b\,\mu\nu}\widetilde{G}^b_{\mu\nu}, \quad (5)$$

where the KSVZ quarks have been assumed to be in the fundamental representation of SU(3)$_c$. For $f_{\rm PQ} = \sqrt{2}v_{\rm PQ}$, one thus recovers the well-known form of the corresponding interaction term as given in (2).[1]

Numerous laboratory, astrophysical, and cosmological studies point to [59, 60]

$$f_{\rm PQ} \gtrsim 6 \times 10^8 \text{ GeV}. \quad (6)$$

This corresponds to an upper limit of about 10 meV on the axion mass,

$$m_a \simeq 6 \text{ meV} \left(\frac{10^9\,\text{GeV}}{f_{\rm PQ}}\right), \quad (7)$$

and implies that axions are stable on cosmological timescales. Because of the larger mass of the saxion, its lifetime τ_σ is typically smaller than the age of the Universe and governed by the following decay widths. From (4) one obtains the width for the saxion decay into axions,[2]

$$\Gamma_{\sigma\to aa} = \frac{x^2 m_\sigma^3}{64\pi v_{\rm PQ}^2} = \frac{x^2 m_\sigma^3}{32\pi f_{\rm PQ}^2}, \quad (8)$$

and from (2) the width for the saxion decay into gluons,

$$\Gamma_{\sigma\to gg} = \frac{\alpha_s^2 m_\sigma^3}{16\pi^3 f_{\rm PQ}^2}. \quad (9)$$

For KSVZ fields that carry an non-zero electrical charge $e_Q e$ with $e = \sqrt{4\pi\alpha}$ and the fine-structure constant α, the saxion can decay into photons via KSVZ quark loops. After integrating out those loops, we find the associated width

$$\Gamma_{\sigma\to\gamma\gamma} = \frac{9e_Q^4\alpha^2 m_\sigma^3}{64\pi^3 f_{\rm PQ}^2}. \quad (10)$$

If $x \gtrsim 0.2$, the saxion decay into axions governs τ_σ, which is the case on which we focus in this work. Indeed, in the region $m_\sigma \gtrsim 1$ GeV in which the competing decay $\sigma \to gg$ is possible, such x values imply the branching ratio BR$(\sigma \to aa) \gtrsim 0.9$. For m_σ below the threshold to form hadrons, where $\sigma \to \gamma\gamma$ is the competing decay, the decay into axions governs τ_σ for even smaller values of x, e.g., for $e_Q = 1$ and $x = 0.02$, we still find the branching ratio BR$(\sigma \to aa) \gtrsim 0.9$.

III. THERMAL SAXION PRODUCTION

Let us now calculate the thermal production of saxions in the primordial SUSY QCD plasma. Assuming that inflation has governed the earliest moments of the Universe, any initial population of saxions has been diluted away by the exponential expansion during the slow-roll phase. After completion of the reheating phase that leads to a radiation-dominated epoch with an initial temperature $T_{\rm R}$, the thermal production of saxions starts to become efficient. In fact, we focus on cosmological settings in which radiation governs the energy density of the Universe as long as this production mechanism is efficient (i.e., for T down to at least $T \sim 0.01\, T_{\rm R}$). While inflation models can point to $T_{\rm R}$ well above 10^{10} GeV, we consider the case $T_{\rm R} < f_{\rm PQ}$ such that no PQ symmetry restoration takes place after inflation. Moreover, $T_{\rm R} < m_{Q,\tilde{Q}}$ is assumed in line with our comments on the considered KSVZ axion model settings in the previous section.

---

[1] Here we focus on $N_Q = 1$ heavy KSVZ (s)quark multiplets Q_L and $\bar{Q}_R$. For $N_Q > 1$, $f_{\rm PQ} \to f_{\rm PQ}/N_Q$, e.g., in (1), (2), (6), and (9) in line with an additional factor of N_Q on the right-hand side of (5). Using this $f_{\rm PQ}$ definition, there are no modifications of the relation $f_{\rm PQ} = \sqrt{2}v_{\rm PQ}$ and of (8) below for $N_Q > 1$.

[2] Our result (8) agrees with the ones of Refs. [10, 39], where $x = 1$ and $f_{\rm PQ} \equiv v_{\rm PQ}$, and of Refs. [11, 61, 62], where $F_a \equiv v_{\rm PQ}$.

The calculation of the thermal production of saxions with $E \gtrsim T$ follows closely [17], where thermal axion production in a SM QGP is considered. From (2) we get the relevant $2 \to 2$ processes shown in Fig. 1. Additional processes exist but can be accounted for by multiplying the squared matrix elements of the shown processes with appropriate multiplicity factors. The squared matrix elements of the shown processes are listed in Table I, where $s = (P_1 + P_2)^2$ and $t = (P_1 - P_3)^2$ with P_1, P_2, P_3, and P referring to the particles in the given order. Working in the limit, $T \gg m_i$, the masses m_i of all MSSM particles involved have been neglected. Sums over initial and final spins have been performed. For quarks and squarks, the contribution of a single chirality is given. The obtained squared matrix elements can be calculated conveniently, e.g., with the help of `FeynArts` [63] and `FormCalc` [64].

The results for processes A, C, E, and G given in Table I point to potential infrared (IR) divergences. Here screening effects of the plasma become relevant. In Ref. [30, 31] a systematic method is introduced to account for such screening effects in a gauge-invariant way. Following Ref. [31], we introduce a momentum scale $k_{\rm cut}$ such that $g_s T \ll k_{\rm cut} \ll T$ in the weak coupling limit $g_s \ll 1$. This separates soft gluons with momentum transfer of order $g_s T$ from hard gluons with momentum transfer of order T. By summing the respective soft and hard contributions, the finite rate for thermal production of saxions with $E \gtrsim T$ is obtained in leading order in g_s,

$$E\frac{dW_\sigma}{d^3p} = E\frac{dW_\sigma}{d^3p}\bigg|_{\rm soft} + E\frac{dW_\sigma}{d^3p}\bigg|_{\rm hard}, \tag{11}$$

which is independent of $k_{\rm cut}$.

In the region where $k < k_{\rm cut}$, we use the optical the-

TABLE I. Squared matrix elements for saxion (σ) production in 2-body processes involving MSSM quarks and squarks of a single chirality (q_i, $\tilde{q}_i$), gluons (g^a), and gluinos ($\tilde{g}^a$) in the high-temperature limit, $T \gg m_i$, with the SU(3)$_c$ color matrices f^{abc} and T^a_{ji}. Sums over initial and final state spins have been performed.

Label i	Process i	$\lvert M_i\rvert^2/\left(\frac{g_s^6}{128\pi^4 f_{\rm PQ}^2}\right)$
A	$g^a + g^b \to g^c + \sigma$	$-4\frac{(s^2+st+t^2)^2}{st(s+t)}\lvert f^{abc}\rvert^2$
B	$q_i + \bar{q}_j \to g^a + \sigma$	$\left(\frac{2t^2}{s} + 2t + s\right)\lvert T^a_{ji}\rvert^2$
C	$q_i + g^a \to q_j + \sigma$	$\left(-\frac{2s^2}{t} - 2s - t\right)\lvert T^a_{ji}\rvert^2$
D	$\tilde{g}^a + \tilde{g}^b \to g^c + \sigma$	$2\left(\frac{2t^2}{s} + 2t + s\right)\lvert f^{abc}\rvert^2$
E	$\tilde{g}^a + g^b \to \tilde{g}^c + \sigma$	$2\left(-\frac{2s^2}{t} - 2s - t\right)\lvert f^{abc}\rvert^2$
F	$\tilde{q}_i + \bar{\tilde{q}}_j \to g^a + \sigma$	$-2\left(\frac{t^2}{s} + t\right)\lvert T^a_{ji}\rvert^2$
G	$\tilde{q}_i + g^a \to \tilde{q}_j + \sigma$	$-2\left(\frac{s^2}{t} + s\right)\lvert T^a_{ji}\rvert^2$
H	$\tilde{q}_i + \bar{q}_j \to \tilde{g}^a + \sigma$	$(s+t)\lvert T^a_{ji}\rvert^2$
I	$\tilde{g}^a + q_i \to \tilde{q}_j + \sigma$	$s\lvert T^a_{ji}\rvert^2$
J	$\tilde{g}^a + \tilde{q}_i \to q_j + \sigma$	$-t\lvert T^a_{ji}\rvert^2$

Process A: $g^a + g^b \to g^c + \sigma$

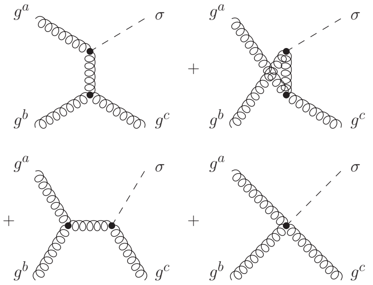

Process B: $q_i + \bar{q}_j \to g^a + \sigma$

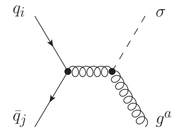

Process C: $q_i + g^a \to q_j + \sigma$ (Crossing of B)

Process D: $\tilde{g}^a + \tilde{g}^b \to g^c + \sigma$

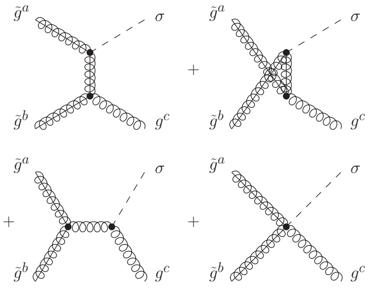

Process E: $\tilde{g}^a + g^b \to \tilde{g}^c + \sigma$ (Crossing of D)

Process F: $\tilde{q}_i + \bar{\tilde{q}}_j \to g^a + \sigma$

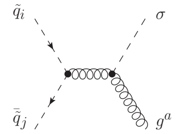

Process G: $\tilde{q}_i + g^a \to \tilde{q}_j + \sigma$ (Crossing of F)

Process H: $\tilde{q}_i + \bar{q}_j \to \tilde{g}^a + \sigma$

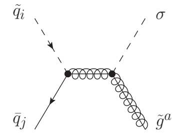

Process I: $\tilde{g}^a + q_i \to \tilde{q}_j + \sigma$ (Crossing of H)

Process J: $\tilde{g}^a + \tilde{q}_i \to q_j + \sigma$ (Crossing of H)

FIG. 1. The $2 \to 2$ processes for saxion production in a SUSY QCD plasma. Additional processes are included in terms of multiplicities in our calculation of the thermal production rate: Process C with antiquarks $\bar{q}_{i,j}$ replacing $q_{i,j}$, process G with antisquarks $\bar{\tilde{q}}_{i,j}$ replacing $\tilde{q}_{i,j}$, process H with antisquarks/quarks $\bar{\tilde{q}}_i/q_j$ replacing $\tilde{q}_i/\bar{q}_j$, and processes I and J with $\bar{q}_i$ and $\bar{\tilde{q}}_j$ replacing q_i and $\tilde{q}_j$, respectively.

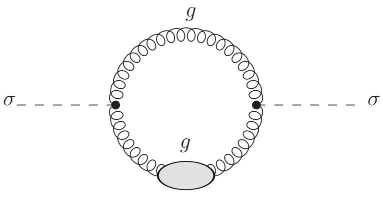

FIG. 2. The saxion self energy used to compute the leading contribution to the thermal production rate of hard saxions. The blob indicates the HTL-resummed gluon propagator.

orem to obtain the soft contribution from the imaginary part of the saxion self energy shown in Fig. 2. Since only one gluon can carry a soft momentum, we need to use the HTL-resummed propagator only once. Using k_{cut} as the ultraviolet cutoff, we get

$$E\frac{dW_\sigma}{d^3p}\bigg|_{\text{soft}} = -\frac{f_{\text{B}}(E)}{(2\pi)^3}\,\text{Im}\,\Pi_\sigma(E+i\epsilon,\vec{p})|_{k<k_{\text{cut}}} \tag{12}$$

$$= E f_{\text{B}}(E)\frac{3m_g^2 g_s^4(N_c^2-1)T}{8192\pi^8 f_{\text{PQ}}^2}\left[\ln\!\left(\frac{k_{\text{cut}}^2}{m_g^2}\right)-1.379\right], \tag{13}$$

where the squared SUSY thermal gluon mass is given by $m_g^2 = g_s^2T^2(N_c+n_f)/6$ for $N_c = 3$ colors and $n_f = 6$ light quark flavors and the equilibrium phase space density for bosons (fermions) by $f_{\text{B(F)}}(E) = [\exp(E/T)\mp 1]^{-1}$. More details on the way in which this calculation is performed can be found in Refs. [31, 32, 35, 36].

In the region where $k > k_{\text{cut}}$ we can use zero temperature Feynman rules since k_{cut} provides an IR cutoff. From the matrix elements given in Table I, weighted with appropriate multiplicities, statistical factors, and phase space distributions, we get the (angle-averaged) hard contribution

$$E\frac{dW_\sigma}{d^3p}\bigg|_{\text{hard}} = \frac{1}{2(2\pi)^3}\int\frac{d\Omega_p}{4\pi}\int\left[\prod_{j=1}^{3}\frac{d^3p_j}{(2\pi)^3 2E_j}\right]$$
$$\times\,(2\pi)^4\delta^4(P_1+P_2-P_3-P)\Theta(k-k_{\text{cut}})$$
$$\times\sum f_1(E_1)f_2(E_2)[1\pm f_3(E_3)]|M_{1+2\to 3+\sigma}|^2 \tag{14}$$

$$= E\frac{g_s^6(N_c^2-1)(N_c+n_f)}{512\pi^7 f_{\text{PQ}}^2}\left\{\frac{f_{\text{B}}(E)T^3}{48\pi}\ln(2)\right.$$
$$+\frac{f_{\text{B}}(E)T^3}{32\pi}\left[\ln\left(\frac{T^2}{k_{\text{cut}}^2}\right)+\frac{17}{3}-2\gamma+\frac{2\zeta'(2)}{\zeta(2)}\right] \tag{15}$$
$$\left.+(I^{(1)}_{\text{BBB}}+I^{(1)}_{\text{FBF}}-I^{(3)}_{\text{BBB}}+I^{(3)}_{\text{FFB}})-2\frac{n_f(I^{(2)}_{\text{FBF}}+I^{(2)}_{\text{FFB}})}{N_c+n_f}\right\}$$

with Euler's constant γ, Riemann's zeta function $\zeta(z)$,

$$I^{(1)}_{\text{BBB(FBF)}} = \frac{1}{32\pi^3E^2}\int_0^\infty dE_3\int_0^{E+E_3}dE_1\ln\left(\frac{|E_1-E_3|}{E_3}\right)$$
$$\times\left\{-\Theta(E_1-E_3)\frac{d}{dE_1}[f_{\text{BBB(FBF)}}E_2^2(E_1^2+E_3^2)]\right.$$
$$+\,\Theta(E_3-E_1)\frac{d}{dE_1}[f_{\text{BBB(FBF)}}E^2(E_1^2+E_3^2)]$$
$$\left.+\Theta(E-E_1)\frac{d}{dE_1}[f_{\text{BBB(FBF)}}(E_1^2E_2^2-E_3^2E^2)]\right\}, \tag{16}$$

$$I^{(2)}_{\text{FBF(FFB)}} = \frac{1}{96\pi^3E^2}\int_0^\infty dE_3\int_0^{E+E_3}dE_2\,f_{\text{FBF(FFB)}}$$
$$\times\left\{\Theta(E-E_3)\left[E_3^2\,(E_3-3E_1)-\Theta(E_2-E)(E_2-E)^3\right]\right.$$
$$+\,\Theta(E_3-E)\left[(E-3E_2)\,E^2+\Theta(E-E_2)(E_2-E)^3\right]$$
$$+\,[\Theta(E_3-E_2)\Theta(E-E_3)-\Theta(E_3-E)\Theta(E_2-E_3)]$$
$$\left.\times\,\left[(E_2-E_3)^2(E_2+2E_3)-3(E_2^2-E_3^2)E\right]\right\}, \tag{17}$$

$$I^{(3)}_{\text{BBB(FFB)}} = \frac{1}{32\pi^3E^2}\int_0^\infty dE_3\int_0^{E+E_3}dE_2\,f_{\text{BBB(FFB)}}$$
$$\times\left\{\Theta(E-E_3)\frac{E_1^2E_3^2}{E_3+E}+\Theta(E_3-E)\frac{E^2E_2^2}{E_3+E}\right.$$
$$+[\Theta(E_3-E)\Theta(E_2-E_3)-\Theta(E-E_3)\Theta(E_3-E_2)]$$
$$\left.\times\,(E_2-E_3)\,[E_2(E_3-E)-E_3(E_3+E)]\right\}, \tag{18}$$

$$f_{\text{BBB,FBF,FFB}} = f_1(E_1)f_2(E_2)[1\pm f_3(E_3)]. \tag{19}$$

The sum in (14) is over all saxion production processes $1+2\to 3+\sigma$ viable with (2). The colored particles 1–3 were in thermal equilibrium at the relevant times. Performing the calculation in the rest frame of the plasma, f_i are thus described by $f_{\text{F/B}}$ depending on the respective spins. Shorthand notation (19) indicates the corresponding combinations, where $+$ ($-$) accounts for Bose enhancement (Pauli blocking) when particle 3 is a boson (fermion). With any initial saxion population diluted away by inflation and for T well below the saxion decoupling temperature T_{D} (which will be determined in Sect.V), we can neglect saxion disappearance reactions and Bose enhancement by saxions, since the saxion phase space density $f_\sigma \ll f_{\text{F/B}}$ and $1+f_\sigma\approx 1$.

IV. THERMAL AXION PRODUCTION

The calculation of thermal axion production in the primordial SUSY QCD plasma proceeds analogously to the saxion calculation presented in the previous section. After substituting the saxion σ by the axion a, the Feynman diagrams can be read directly from Figs. 1 and 2 with one modification: there is no gluino-gluino-gluon-axion vertex and thus no quartic interaction such as the one that contributes to processes D and E in the saxion case.

Although the Feynman rules for the axion interactions derived from (2) differ from the ones describing saxion interactions, we obtain squared matrix elements for the axion production processes in the high-temperature limit, $T \gg m_i$, that agree with the ones for the corresponding saxion production processes given in Table I. Moreover, we find that both the soft and the hard contributions to the thermal production rate of hard axions agree with (13) and (15), respectively. Our result for the thermal axion production rate $E\,dW_a/d^3p$ thus agrees with the one for the thermal saxion production rate obtained above. This implies an agreement of the associated thermally produced yields of axions and saxions prior to decay, which will be calculated in the next section.

Before proceeding let us stress that we can neglect production processes like $\pi\pi \to \pi a$ in the primordial hot hadronic gas [14, 16] because of the $f_{\rm PQ}$ limit (6). Moreover, Primakoff processes such as $e^-\gamma \to e^- a$ are not taken into account since they are usually far less efficient in the early Universe [13].

V. THERMAL SAXION/AXION YIELD

Let us now calculate the thermally produced (TP) saxion yield $Y_\sigma^{\rm TP} = n_\sigma/s$, where n_σ is the corresponding saxion number density and s the entropy density. With the results obtained in the two previous sections, we know beforehand that this yield prior to decay agrees with the thermally produced axion yield $Y_a^{\rm TP} = n_a/s$. While the calculation and results are indeed valid for both saxion and axion, we focus on the saxion case.

For T sufficiently below the saxion decoupling temperature $T_{\rm D}$, the evolution of the thermally produced n_σ with cosmic time t is governed by the Boltzmann equation

$$\frac{dn_\sigma}{dt} + 3Hn_\sigma = \int d^3p\,\frac{dW_\sigma}{d^3p} = W_\sigma. \qquad (20)$$

Here H is the Hubble expansion rate, and the collision term is the integrated thermal production rate:

$$W_\sigma = \frac{9\zeta(3)g_s^6 T^6}{256\pi^7 f_{\rm PQ}^2}\left[\ln\left(\frac{T^2}{m_g^2}\right) + 0.4305\right]. \qquad (21)$$

Assuming conservation of entropy per comoving volume element, (20) can be written as $dY_\sigma^{\rm TP}/dt = W_\sigma/s$. Since thermal saxion production is efficient only in the hot radiation dominated epoch with temperatures well above the one of radiation-matter equality, $T_{\rm mat=rad}$, we can change variables from cosmic time t to temperature T accordingly. With an initial temperature $T_{\rm R}$ at which $Y_\sigma^{\rm TP}(T_{\rm R}) \simeq 0$, the relic saxion yield prior to decay is

$$\begin{aligned} Y_\sigma^{\rm TP} &\approx Y_\sigma^{\rm TP}(T_{\rm low}) = \int_{T_{\rm low}}^{T_{\rm R}} dT\,\frac{W_\sigma(T)}{T s(T) H(T)} \\ &= 1.33\times 10^{-3} g_s^6 \ln\!\left(\frac{1.01}{g_s}\right)\!\left(\frac{10^{11}\,{\rm GeV}}{f_{\rm PQ}}\right)^{\!2}\!\left(\frac{T_{\rm R}}{10^8\,{\rm GeV}}\right) \end{aligned} \qquad (22)$$

with a fiducial temperature $T_{\rm low}$ well below $T_{\rm R}$ and well above T_σ, which we use to denote the temperature of the primordial plasma at $t = \tau_\sigma$: $T_\sigma \ll T_{\rm low} \ll T_{\rm R}$. In the case of the axion, $T_{\rm low} = T_{\rm mat=rad}$ can be used since its lifetime exceeds the time of radiation-matter equality significantly. Note that the resulting saxion/axion yield is insensitive to the exact choice of $T_{\rm low}$ for $T_{\rm low} < 0.01\,T_{\rm R}$ since additional contributions from thermal production at $T < 0.01\,T_{\rm R}$ are found to be negligible.

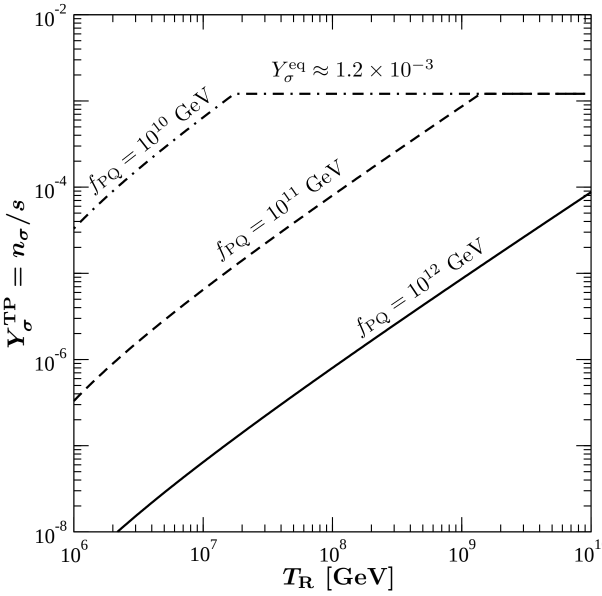

FIG. 3. The relic saxion yield prior to decay originating from thermal processes in the primordial plasma for cosmological scenarios characterized by different $T_{\rm R}$ values covering the range from 10^6 to 10^{10} GeV. The dash-dotted, dashed, and solid lines are obtained for $f_{\rm PQ} = 10^{10}$, 10^{11}, and 10^{12} GeV. The relic axion yield $Y_a^{\rm eq/TP}$ from thermal processes agrees with $Y_\sigma^{\rm eq/TP}$ and can thus be read from this figure as well.

Figure 3 shows the saxion yield (22) for $f_{\rm PQ} = 10^{10}$, 10^{11}, and 10^{12} GeV as the diagonal dash-dotted, dashed, and solid lines, respectively. Here we compute (22) with $g_s \equiv g_s(T_{\rm R}) = \sqrt{4\pi\alpha_s(T_{\rm R})}$ evaluated according to its 1-loop renormalization group running within the MSSM from $\alpha_s(m_{\rm Z}) = 0.1176$ at the Z-boson mass $m_{\rm Z} = 91.1876$ GeV. The applied methods [30, 31] require $g_s \ll 1$, so that (22) is most reliable for $T_{\rm R} \gg 10^6$ GeV. For lower $T_{\rm R}$ values such that $g_s(T_{\rm R}) \gtrsim 1$, one encounters an artificial suppression of $Y_\sigma^{\rm TP}$ and even unphysical negative values, which can be seen directly from the logarithmic factor in (22). This is a well-known limitation of this technique (cf. [17, 24]) that calls for generalizations of the gauge-invariant methods introduced in Refs. [30, 31] modified to extend the applicability beyond the weak coupling limit.

Note that (22) is only valid if $T_{\rm R} \ll T_{\rm D}$, because otherwise saxion annihilation processes neglected in (14) are important. For $T_{\rm R} \gtrsim T_{\rm D}$ saxions were in thermal equilibrium in the early Universe before decoupling as thermal relics. In fact, for $m_\sigma \ll T_{\rm D}$, saxions decouple as a relativistic species. The yield is then given by

$$Y_\sigma^{\rm eq} = \frac{n_\sigma^{\rm eq}}{s} \approx 1.2 \times 10^{-3} \qquad (23)$$

as indicated by the horizontal lines in Fig. 3. The yield from thermal production cannot exceed the equilibrium yield, so that (23) represents an upper limit. In scenarios with values of $T_{\rm R}$ for which (22) is equal or larger than (23), saxion disappearance reactions have to be taken into account. The resulting yield would show almost the same $T_{\rm R}$ dependence as the one in Fig. 3, but with a smooth transition in the $T_{\rm R}$ range in which $Y_\sigma^{\rm TP} \simeq Y_\sigma^{\rm eq}$.

For axions, $m_a \ll T_{\rm D}$ is always satisfied so that they will be hot thermal relics with $Y_a^{\rm eq} = Y_\sigma^{\rm eq}$ as given in (23) if $T_{\rm R} \gtrsim T_{\rm D}$. In fact, the relic axion yield $Y_a^{\rm eq/TP}$ from thermal processes agrees fully with $Y_\sigma^{\rm eq/TP}$described above and can be read from Fig. 3 as well.

VI. DECOUPLING TEMPERATURE

Considering Fig. 3, one finds that the kinks indicate critical $T_{\rm R}$ values. For a given $f_{\rm PQ}$, the associated critical $T_{\rm R}$ value separates scenarios with thermal relic saxions from those in which saxions have never been in thermal equilibrium. We thus use the positions of the kinks as $f_{\rm PQ}$-dependent estimates of the saxion decoupling temperature. Our numerical results are well described by

$$T_{\rm D} \approx 1.4 \times 10^9 \text{ GeV} \left(\frac{f_{\rm PQ}}{10^{11} \text{ GeV}}\right)^2 . \qquad (24)$$

This is similar to the estimate of the axino decoupling temperature in Ref. [19]. Such an agreement was expected and used to provide estimates of the thermally produced saxion yield $Y_\sigma^{\rm TP}$ in Refs. [10, 11, 22, 39]. Another recent study applies the thermally produced axino yield $Y_{\tilde a}^{\rm TP}$ [24] to estimate $Y_\sigma^{\rm TP} \simeq (2/3)\, Y_{\tilde a}^{\rm TP}$ [62].[3] With our results illustrated in Fig. 3 above, one can now see explicitly the similarity between $Y_\sigma^{\rm TP}$ and the corresponding axino yield $Y_{\tilde a}^{\rm TP}$ illustrated in Fig. 4 of Ref. [24].

In light of Sect. IV, it is clear that (24) describes the axion decoupling temperature in the considered SUSY settings as well. When comparing (24) with the axion decoupling temperature in non-SUSY scenarios, given in Eq. (15) of Ref. [17], we find only small differences. In fact, for a fixed $g_s \ll 1$, the additional diagrams in the SUSY case (which lead to a different thermal gluon mass m_g also) increase the collision term for thermal axion production W_a only by at most 30% with respect to Eq. (12) of Ref. [17] obtained for the non-SUSY case. Note also that both $Y_a^{\rm TP}$ and $Y_a^{\rm eq}$ are normalized to an entropy density $s(T)$ which is more than two times larger in the SUSY case than in the non-SUSY case due to the additional sparticles which can all be considered to be relativistic at very high temperatures such as the axion decoupling temperature.

VII. ADDITIONAL RADIATION FROM SAXION DECAYS

As already mentioned in the Introduction, axions from late saxion decays can provide additional radiation already prior to BBN and later on as well. The amount of additional radiation is usually expressed in terms of a non-standard contribution $\Delta N_{\rm eff}$ to the effective number of light thermally excited neutrino species $N_{\rm eff}$. It is defined in relation to the total relativistic energy density

$$\rho_{\rm rad}(T) = \left[1 + \frac{7}{8} N_{\rm eff} \left(\frac{T_\nu}{T}\right)^4\right] \rho_\gamma(T) \qquad (25)$$

with the photon energy density ρ_γ and the temperatures of neutrinos T_ν and of photons T. At $T \gtrsim$ 1 MeV (before neutrino decoupling and e^+e^- annihilation), $N_{\rm eff} = 3 + \Delta N_{\rm eff}$ and $T_\nu = T$. These relations change to $T_\nu = (11/4)^{-1/3} T$ after neutrino decoupling and to $N_{\rm eff} = 3.046 + \Delta N_{\rm eff}$ [65] because of residual neutrino heating by e^+e^- annihilation.

At a photon temperature $T < T_\sigma$, the energy density of relativistic non-thermally produced (NTP) axions from saxion decays $\rho_a^{\rm NTP}(T)$ yields

$$\Delta N_{\rm eff}(T) = \frac{120}{7\pi^2 T_\nu^4}\, \rho_a^{\rm NTP}(T). \qquad (26)$$

Working in the sudden decay approximation, all thermally produced saxions are considered to decay instantaneously at $t = \tau_\sigma$ (where $T = T_\sigma$). If the saxions are non-relativistic when decaying dominantly into two axions, the initial axion momentum is $p_a(T_\sigma) = m_\sigma/2$ and

$$\begin{aligned}\rho_a^{\rm NTP}(T) &= \frac{m_\sigma}{2} \left[\frac{g_{*S}(T)}{g_{*S}(T_\sigma)}\right]^{1/3} \frac{T}{T_\sigma}\, Y_a^{\rm NTP} s(T) &(27)\\ &= \left[\frac{g_{*S}(T)}{g_{*S}(T_\sigma)}\right]^{4/3} \left(\frac{T}{T_\sigma}\right)^4 \rho_\sigma^{\rm eq/TP}(T_\sigma) &(28)\end{aligned}$$

with $\rho_\sigma^{\rm eq/TP}(T_\sigma) = m_\sigma Y_\sigma^{\rm eq/TP} s(T_\sigma)$ and $Y_a^{\rm NTP} = 2 Y_\sigma^{\rm eq/TP}$. Here g_{*S} denotes the number of effectively massless degrees of freedom such that $s = 2\pi^2 g_{*S} T^3/45$. For $\tau_\sigma \simeq 1/\Gamma_{\sigma\to aa}$ given by (8) and with the time-temperature relation in the radiation-dominated epoch, we obtain

$$T_\sigma \simeq 10.6 \text{ MeV} \left(\frac{m_\sigma}{1 \text{ GeV}}\right)^{3/2} \left(\frac{10^{10}\text{ GeV}}{f_{\rm PQ}/x}\right) \left[\frac{10.75}{g_*(T_\sigma)}\right]^{1/4} \qquad (29)$$

---

[3] Note that $f_{\rm PQ}$ in [10, 39] and F_a in [11, 62] correspond to our $v_{\rm PQ} = f_{\rm PQ}/\sqrt{2}$ and thereby differ by $1/\sqrt{2}$ from our $f_{\rm PQ}$. With these differences in the definitions of the PQ scale, we find that the $Y_\sigma^{\rm TP}$ estimates in Refs. [10, 11, 39, 62] exceed the result (22) of our calculation by about a factor of two for fixed $f_{\rm PQ}$ and $T_{\rm R}$.

and

$$\Delta N_{\rm eff}(T) \simeq \frac{0.95}{x}\left(\frac{100\ \mathrm{GeV}}{m_\sigma}\right)^{1/2}\left(\frac{f_{\rm PQ}}{10^{11}\,\mathrm{GeV}}\right)\left(\frac{Y_\sigma^{\rm eq/TP}}{10^{-3}}\right) \times\left(\frac{T}{T_\nu}\right)^4\left[\frac{g_{*S}(T)}{10.75}\right]^{4/3}\frac{g_*(\tau_\sigma)^{1/4}}{g_{*S}(\tau_\sigma)^{1/3}}, \tag{30}$$

where g_* is the effective number of relativistic degrees of freedom governing the energy density.

Focussing on saxions from thermal processes, the maximum $\Delta N_{\rm eff}$ emerges for scenarios with $T_{\rm R}$ above the decoupling temperature (24) so that the thermal relic yield (23) applies:

$$\Delta N_{\rm eff}(T) \simeq \frac{1.14}{x}\left(\frac{100\ \mathrm{GeV}}{m_\sigma}\right)^{1/2}\left(\frac{f_{\rm PQ}}{10^{11}\,\mathrm{GeV}}\right) \times\left(\frac{T}{T_\nu}\right)^4\left[\frac{g_{*S}(T)}{10.75}\right]^{4/3}\frac{g_*(\tau_\sigma)^{1/4}}{g_{*S}(\tau_\sigma)^{1/3}}. \tag{31}$$

For $T_{\rm R} < T_{\rm D}$ on the other hand, the yield (22) leads to:

$$\Delta N_{\rm eff}(T) \simeq \frac{12.6 g_s^6 \ln\left(\frac{1.01}{g_s}\right)}{x}\left(\frac{1\ \mathrm{GeV}}{m_\sigma}\right)^{1/2}\left(\frac{10^{11}\,\mathrm{GeV}}{f_{\rm PQ}}\right) \times\left(\frac{T_{\rm R}}{10^8\,\mathrm{GeV}}\right)\left(\frac{T}{T_\nu}\right)^4\left[\frac{g_{*S}(T)}{10.75}\right]^{4/3}\frac{g_*(\tau_\sigma)^{1/4}}{g_{*S}(\tau_\sigma)^{1/3}}. \tag{32}$$

Thermal relic saxions are non-relativistic when decaying if their average momentum at T_σ satisfies

$$\langle p(T_\sigma)\rangle = \langle p(T_{\rm D})\rangle\left[\frac{g_{*S}(T_\sigma)}{g_{*S}(T_{\rm D})}\right]^{1/3}\frac{T_\sigma}{T_{\rm D}} \ll m_\sigma. \tag{33}$$

Since those saxions decouple as a relativistic species (provided $m_\sigma \ll T_{\rm D}$) at a very high temperature (24) with a thermal spectrum, $\langle p(T_{\rm D})\rangle = 2.701\,T_{\rm D}$ and $g_{*S}(T_{\rm D}) \simeq 232.5$.[4] Using (29), we can express (33) in terms of the following m_σ-dependent lower limit on the PQ scale

$$\frac{f_{\rm PQ}}{x} \gg 8.4\times 10^7\,\mathrm{GeV}\left(\frac{m_\sigma}{1\ \mathrm{GeV}}\right)^{1/2}\frac{g_{*S}(T_\sigma)^{1/3}}{g_*(T_\sigma)^{1/4}}. \tag{34}$$

Almost the same limit applies to thermally produced saxions as well since their production is efficient only at high temperatures not far below $T_{\rm R}$ and leads basically to a thermal spectrum, i.e., (33) applies after substituting $T_{\rm D}$ by $T_{\rm R}$ and $g_{*S}(T_{\rm D})$ by $g_{*S}(T_{\rm R}) \simeq 228.75$.

Note that the saxions decay while being decoupled from the primordial plasma if $T_\sigma \ll T_{\rm D}$ or equivalently

$$\frac{f_{\rm PQ}}{x^{1/3}} \gg 7.1\times 10^7\,\mathrm{GeV}\left(\frac{m_\sigma}{100\ \mathrm{GeV}}\right)^{1/2}\left[\frac{232.5}{g_*(T_\sigma)}\right]^{1/12}. \tag{35}$$

If this condition is satisfied the axions emitted in those decays will not be thermalized and be free-streaming. Thus, the temperature $T_{\rm nr}$ at which the non-thermally produced axions become non-relativistic reads

$$T_{\rm nr} = 0.15\,x\ \mathrm{eV}\left(\frac{m_\sigma}{10\ \mathrm{TeV}}\right)^{1/2}\left(\frac{10^9\,\mathrm{GeV}}{f_{\rm PQ}}\right)^2 \times\left[\frac{3.91}{g_{*S}(T_{\rm nr})}\right]^{1/3}\frac{g_{*S}(T_\sigma)^{1/3}}{g_*(T_\sigma)^{1/4}}, \tag{36}$$

when defined via $p_a(T_{\rm nr}) = m_a$. This shows that the emitted axions are expected to be still relativistic at the last scattering surface and even well thereafter for $m_\sigma \lesssim 10$ TeV and $x = \mathcal{O}(1)$. Thereby they can contribute to $\Delta N_{\rm eff}$ even at late times where studies of the CMB and LSS allow us to probe the amount of radiation.

A. BBN

For $T_\sigma \gtrsim 1$ MeV, the axions from saxion decays contribute to the radiation density already at the onset of BBN and prior to e^+e^- annihilation. This leads to a speed-up of the Hubble expansion rate and thereby to an output of ^{4}He that is more efficient than in standard BBN with $\Delta N_{\rm eff} = 0$. In turn, the inferred primordial ^{4}He abundance imposes upper limits on $\Delta N_{\rm eff}$, whereas the inferred primordial D abundance constrains the baryon density $\omega_{\rm b} = \Omega_{\rm b}h^2$, with the normalized Hubble constant $h \simeq 0.7$. Notably, two recent studies of the primordial ^{4}He mass fraction $Y_{\rm p}$ even report values in excess by more than 2σ over the standard BBN prediction: Izotov and Thuan [46] find $Y_{\rm p}^{\rm IT} = 0.2565 \pm 0.001(\mathrm{stat.}) \pm 0.005(\mathrm{syst.})$ and Aver *et al.* [47] $Y_{\rm p}^{\rm Av} = 0.2561 \pm 0.0108$, with all errors refering to 68% intervals. As mentioned in the Introduction, these results may be hints towards extra radiation at the onset of BBN, which can reside in the form of axions from decays of saxions from thermal processes.

Based on recent studies of the primordial ^{4}He and D abundances [46, 47, 66] and the recent Particle Data Group (PDG) recommendation for the free neutron lifetime, $\tau_{\rm n} = 880.1 \pm 1.1$ s [60], we now derive $\Delta N_{\rm eff}$ limits from a BBN likelihood analysis, similar to the one in Ref. [67], and explore the implications for the considered SUSY axion models. Relying on the $Y_{\rm p}$ results given above and on the primordial D abundance reported by Petini *et al.* [66], $\log[\mathrm{D/H}]_{\rm p} = -4.56 \pm 0.04$, we consider the two log-likelihood functions

$$\ln L_{^4\mathrm{He}} = \begin{cases} -\frac{1}{2}\frac{(Y_{\rm p}-0.2565)^2}{0.0051^2} & \text{for [46]} \\ -\frac{1}{2}\frac{(Y_{\rm p}-0.2561)^2}{0.0108^2} & \text{for [47]} \end{cases} \tag{37}$$

$$\ln L_{\rm D} = -\frac{1}{2}\frac{(\log[\mathrm{D/H}]_{\rm p}+4.56)^2}{0.04^2}, \tag{38}$$

where small uncertainties related to nuclear reaction rates and also the ones related to the free neutron lifetime $\tau_{\rm n}$ are not taken into account. Theoretical values for the primordial ^{4}He and D abundances are calculated with

---

[4] This g_{*S} value accounts for the MSSM and the axion multiplet fields, which can all be considered as relativistic at $T_{\rm D}$ if not only m_σ but also the axino mass satisfies $m_{\tilde a} \ll T_{\rm D}$.

TABLE II. Constraints on $\Delta N_{\rm eff}$ from BBN and precision cosmology. Based on the indicated data sets, the first two lines give the posterior maximum (p.m.) and the minimal 99.7% credible interval imposed by BBN using the prior $\Delta N_{\rm eff} \geq 0$ and after marginalization over $\omega_{\rm b}$. The third line quotes the mean and the 95% CL upper limit on $\Delta N_{\rm eff}$ as obtained in the precision cosmology study of Ref. [48] based on CMB data, the Sloan Digital Sky Survey (SDSS) data-release 7 halo power spectrum (HPS), and data from the Hubble Space Telescope (HST).

Data	p.m./mean	upper limit
$Y_{\rm p}^{\rm IT}$ [46] + $[{\rm D/H}]_{\rm p}$ [66]	0.76	< 1.97 (3σ)
$Y_{\rm p}^{\rm Av}$ [47] + $[{\rm D/H}]_{\rm p}$ [66]	0.77	< 3.53 (3σ)
CMB + HPS + HST [48]	1.73	< 3.59 (2σ)

the BBN code `PArthENoPE` [68] using $\tau_{\rm n} = 880.1$ s [60] and $0 \leq \Delta N_{\rm eff} \leq 4$ and $0.01 \leq \omega_{\rm b} \leq 0.03$ as flat priors. Calculating the respective combined likelihood and after marginalizing over $\omega_{\rm b}$, we obtain for $\Delta N_{\rm eff}$ the maximum likelihood posteriors and the minimal 99.7% credible intervals listed in the first two lines of Table II.[5]

Let us now apply these BBN constraints to the case of extra radiation from saxion decays into axions. We evaluate $\Delta N_{\rm eff}(T)$ from (31) and (32) for $x = 1$ and at $T \sim 1$ MeV, i.e., at the onset of BBN and above the temperature at which neutrinos decouple. Figure 4 shows the resulting $\Delta N_{\rm eff}$ contours in the m_σ–$f_{\rm PQ}$ parameter plane as black (gray) lines for $T_{\rm R} = 10^8$ (10^{10}) GeV. The solid (dashed) curves show – as labeled – the posterior maximum $(\Delta N_{\rm eff})^{\rm p.m.}_{\rm Av(IT)} = 0.77$ (0.76) and the upper limit $(\Delta N_{\rm eff})^{3\sigma}_{\rm Av(IT)} = 3.53\,(1.97)$, which disfavors the considered region to its left by more than 3σ. The dotted lines indicate $T_\sigma = 1$ and 10 MeV. The parameter region with $T_\sigma < 1$ MeV is not considered since our BBN constraints on $\Delta N_{\rm eff}$ do not apply to later decays.[6] Moreover, as described in the Introduction, additional cosmological constraints can occur for $T_\sigma < 1$ MeV, which are beyond the scope of this work.

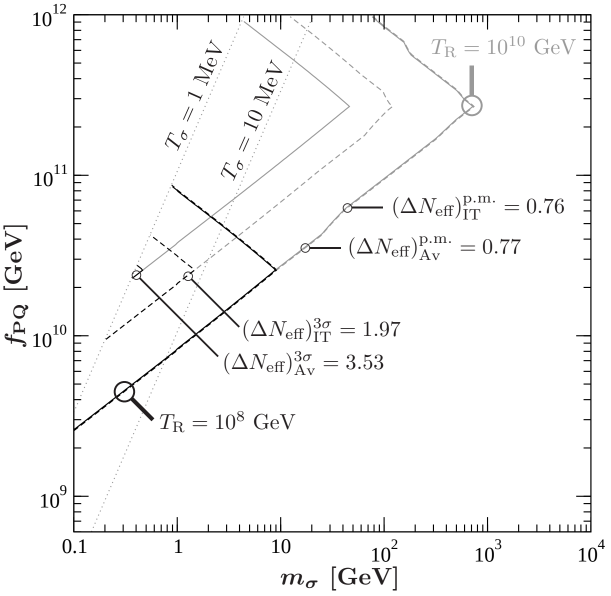

FIG. 4. Contours of $\Delta N_{\rm eff}$ at $T \sim 1$ MeV provided by non-thermally produced axions from decays of thermal saxions for $x = 1$, $T_\sigma > 1$ MeV, and $T_{\rm R} = 10^8$ GeV (black) and 10^{10} GeV (gray). The BBN results given in Table II are illustrated by the solid (dashed) curves, which indicate the posterior maximum $(\Delta N_{\rm eff})^{\rm p.m.}_{\rm Av(IT)} = 0.77$ (0.76) and the upper 3σ limit $(\Delta N_{\rm eff})^{3\sigma}_{\rm Av(IT)} = 3.53$ (1.97) that disfavors the region to its left. The dotted lines show $T_\sigma = 1$ and 10 MeV.

For $T_\sigma > 1$ MeV, one sees that the BBN constraints on $\Delta N_{\rm eff}$ can disfavor significant regions of the m_σ–$f_{\rm PQ}$ parameter plane in high $T_{\rm R}$ scenarios. These regions will become larger and move towards larger m_σ if x is smaller than one but still sufficiently sizable such that the saxion decay into axions remains to be the dominant decay channel that governs τ_σ. Moreover, the shown posterior-maxima contours illustrate that non-thermally produced axions from decays of thermal saxions can explain the existence of extra radiation, $\Delta N_{\rm eff} \sim 1$, in agreement with the hints from BBN studies. For $T_{\rm R} > T_{\rm D}$, the shape of the $\Delta N_{\rm eff}$ contours is described by (31) from decays of thermal relic saxions. The kink of the $\Delta N_{\rm eff}$ contours indicates the respective $f_{\rm PQ}$ value at which $T_{\rm R} = T_{\rm D}$. For larger $f_{\rm PQ}$, $T_{\rm R} < T_{\rm D}$ and (32) applies which is reflected by the $T_{\rm R}$ dependence of $\Delta N_{\rm eff}$ provided by axions from decays of thermally produced saxions.

As mentioned in the Introduction, the energy density of the early Universe can receive contributions not only from thermal saxions but also from coherent oscillations of the saxion field [8–12]. In fact, axions from the decay of those non-thermal saxions constitute additional radiation as well [11, 12] and can thereby increase $\Delta N_{\rm eff}$ already at the onset of BBN. However, in the parameter region considered in Fig. 4, their contribution to $\Delta N_{\rm eff}$ is basically negligible for an initial displacement of the saxion field from the vacuum of $\sigma_i \sim f_{\rm PQ}$. This can be seen, for example, in Fig. 1 of Ref. [11] where the energy density of coherent saxion oscillations is compared with an estimate of the one of thermal saxions.

At this point, it is important to stress that significant additional restrictions are possible that depend on the mass spectrum and on other aspects of the specific SUSY model possibly realized in nature. Here the masses of the axino and the gravitino are of particular importance since their thermal production can be very efficient in high $T_{\rm R}$ scenarios such as those explored in Fig. 4.

---

[5] Note that the PDG-recommended value for the free neutron lifetime has changed recently from $\tau_{\rm n} = 885.7 \pm 0.8$ s [69] to $\tau_{\rm n} = 880.1 \pm 1.1$ s [60]. If we use $\tau_{\rm n} = 885.7$ s in `PArthENoPE`, we can reproduce the posterior maxima and the minimal 95% credible intervals given in the first two lines of Table III in Ref. [70]. In comparison, those posterior maxima are about 10% below the values obtained with $\tau_{\rm n} = 880.1$ s given in our Table II.

[6] The calculations of `PArthENoPE` start at $T = 10$ MeV with the given $\Delta N_{\rm eff}$ values as input already at that temperature. The $\Delta N_{\rm eff}$ limits derived above are thus strictly applicable for $T_\sigma \geq 10$ MeV only. Modifications in the `PArthENoPE` code that will allow us to describe more accurately the region with $T_\sigma < 10$ MeV are postponed to future work.

For example, in R-parity conserving scenarios in which the gravitino is the lightest SUSY particle (LSP), the thermally produced gravitino density is limited from above by the dark matter density parameter $\omega_{\rm CDM} = \Omega_{\rm CDM}h^2 \simeq 0.1$ [60]. This disfavors $T_{\rm R} \gtrsim 10^{10}\,$GeV and translates into $m_{3/2} \lesssim 10$ GeV for $T_{\rm R} = 10^8\,$GeV and universal gaugino masses at the scale of grand unification of $m_{1/2} \sim 0.5$ TeV; cf. Fig. 2 in Ref. [34]. For $m_\sigma \sim m_{3/2}$, as expected in gravity-mediated SUSY breaking, this cosmological constraint will then challenge the $\Delta N_{\rm eff} \sim 1$ explanation presented in Fig. 4 for $T_{\rm R} = 10^8\,$GeV and disfavor the one for $T_{\rm R} = 10^{10}\,$GeV. Depending on the next-to-lightest SUSY particle (NLSP), even more restrictive upper limits on $T_{\rm R}$ are possible; cf. [37] and references therein. Additional limits related to axino cosmology can be evaded, e.g., for $m_{\tilde a} \gtrsim 2$ TeV, a gluino mass of $m_{\tilde g} \sim 1$ TeV, and $f_{\rm PQ} \sim 10^{10}\,$GeV. Although possibly somewhat contrived from the model building point of view, the heavy axinos then decay typically before the NLSP freeze-out and the emitted sparticles will be thermalized such that the constraints associated with the NLSP will not be tightened. If a sneutrino is the NLSP (for which the NLSP-related constraints are rather mild [71–73]), the shown $\Delta N_{\rm eff} \sim 1$ explanation for $T_{\rm R} = 10^8\,$GeV can thereby turn out to be viable for $m_\sigma \sim m_{3/2} \sim 10$ GeV, where cold dark matter can reside in thermally produced gravitinos.

In the alternative axino LSP case, one often finds more restrictive $T_{\rm R}$ constraints imposed by the dark matter constraint [23–25, 74] and also additional $f_{\rm PQ}$ constraints depending on the properties of the NLSP [74–76]. Interestingly, these $T_{\rm R}$ constraints can be avoided in the case of a light axino LSP with $m_{\tilde a} < 0.2\,$keV (cf. Fig. 6 in [24]). Moreover, additional $T_{\rm R}$ constraints from BBN-imposed limits on hadronic/electromagnetic energy injection from late decaying gravitinos can be evaded if the gravitino is the NLSP [22, 77]. In such a setting, the lifetime of the gravitino NLSP is $\tau_{3/2} \sim 10^9\,{\rm s}\,(10^2\,{\rm GeV}/m_{3/2})^3$ and governed by its decay into the axino LSP and an axion [22, 77]. While both of which are too weakly interacting to reprocess primordial nuclei, the emitted particles can contribute to $\Delta N_{\rm eff}$ at cosmic times $t > \tau_{3/2}$ [61]. Upper limits on $\Delta N_{\rm eff}$ imposed by CMB + LSS studies have thereby been found to imply $T_{\rm R} \lesssim 10^{11}\,$GeV at the 5σ level for $m_{3/2} = 100$ GeV and $m_{\tilde g} \sim 1$ TeV [78]. This limit can be overly conservative since it does not include $\Delta N_{\rm eff}$ from saxion decays into axions. For $m_{\tilde g} \sim 1$ TeV, which is still allowed by the ongoing LHC sparticle searches, $m_{3/2} \sim 100$ GeV, and $T_{\rm R} \sim 10^{10}\,$GeV, gravitino decays into axions and axinos have been found to lead to $\Delta N_{\rm eff} \sim 0.6$ but only at times well after the BBN epoch [61, 78]. Taking into account the additional contribution to $\Delta N_{\rm eff}$ at such late times from saxion decays (which we consider explicitly below), we find that this point in parameter space remains to be allowed. This implies viability of the corresponding explanation of $\Delta N_{\rm eff} \sim 1$ at the onset of BBN for $T_{\rm R} = 10^{10}\,$GeV shown in Fig. 4. Here one can easily accommodate also the small additional contribution of $\Delta N_{\rm eff} \lesssim 0.017$ provided by light thermal axinos at the onset of BBN [76]. For $f_{\rm PQ} \sim 10^{12}\,$GeV, cold dark matter can then reside in the form of an axion condensate (cf. Fig. 7 below) whereas axinos will be hot dark matter [24] with associated LSS constraints imposing $m_{\tilde a} \lesssim 37$ eV [76]. While the lightest ordinary sparticle (LOSP) can still be long lived, BBN constraints related to its decay can be evaded. For the stau LOSP case, this is illustrated explicitly in Fig. 21 of Ref. [76]. Thereby, one arrives at viable scenarios with different $\Delta N_{\rm eff}$ predictions at the onset of BBN and much later, in which even $T_{\rm R} \sim 10^{10}\,$GeV is possible, e.g., allowing for the explanation of the baryon asymmetry via thermal leptogenesis [79].

B. CMB and LSS

Axions from saxion decays can contribute to $\Delta N_{\rm eff}$ at the CMB decoupling epoch, even for $T_\sigma \gtrsim 1$ MeV, as described below (36). Extra radiation at that epoch delays the time of radiation-matter equality and is probed by studies of the CMB anisotropies and the LSS distribution. Here hints towards $N_{\rm eff} \gtrsim 3$ have been found that are more pronounced than those from BBN considered above; see [48–52] and references therein. For example, the Wilkinson Microwave Anisotropy Probe (WMAP) collaboration finds a 68% credible interval of $N_{\rm eff} = 4.34^{+0.86}_{-0.88}$ [51] when combining their 7-year data with measurements of the baryonic acoustic oscillation (BAO) scale and todays Hubble constant H_0. Another precision cosmology study arrives at a 95% credible interval of $N_{\rm eff} = 4.78^{+1.86}_{-1.75}$ [48] when combining CMB data with data from the Sloan Digital Sky Survey data-release 7 halo power spectrum (HPS) and the Hubble Space Telescope (HST). Based on this combined CMB + HPS + HST data set, we use the mean for $\Delta N_{\rm eff}$ and the 95% CL upper limit on $\Delta N_{\rm eff}$, as quoted in Table II, to explore implications for the considered SUSY axion models.

Evaluating $\Delta N_{\rm eff}(T)$ from (31) and (32) for $x = 1$ and at $T \ll 1$ MeV,[7] we obtain the $\Delta N_{\rm eff}$ contours for $T_{\rm R} = 10^8\,(10^{10})\,$GeV as shown by the black (gray) lines in Fig. 5. The solid lines indicate the upper limit $\Delta N_{\rm eff} = 3.59$ with the m_σ–$f_{\rm PQ}$ parameter regions to their left disfavored at the 2σ level by the CMB + HPS + HST data set. The dashed lines show the corresponding mean

---

[7] Note that our theoretical results for $\Delta N_{\rm eff}(T)$ at $T \sim 1$ MeV and at $T \ll 1$ MeV agree. The T dependence in (31) and (32) results from the factor $(T/T_\nu)^4[g_{*S}(T)/10.75]^{4/3}$. This factor equals one for $T \sim 1$ MeV, where $T_\nu = T$ and $g_{*S}(T) = 10.75$, and for $T \ll 1$ MeV, where $T_\nu = (11/4)^{-1/3}T$ and $g_{*S}(T) = 3.91$.

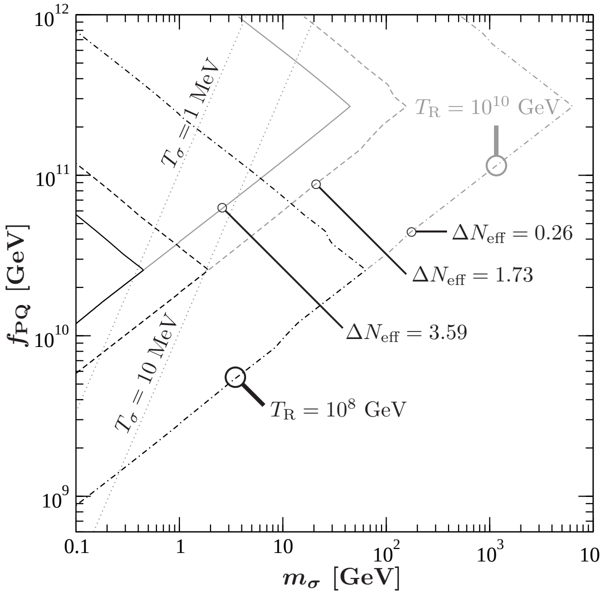

FIG. 5. Contours of ΔN_{eff} at $T \ll 1$ MeV provided by non-thermally produced axions from decays of thermal saxions for $x = 1$ and $T_{\mathrm{R}} = 10^8$ GeV (black) and 10^{10} GeV (gray). The solid curve shows the 2σ limit $\Delta N_{\mathrm{eff}} = 3.59$ and the dashed curve the mean $\Delta N_{\mathrm{eff}} = 1.73$ based on the CMB + HPS + HST result [48] quoted in Table II. The dash-dotted curve indicates $\Delta N_{\mathrm{eff}} = 0.26$ which is the expected 68% CL sensitivity of the Planck satellite mission [53, 54]. On the dotted lines, $T_\sigma = 1$ and 10 MeV, as in Fig. 4.

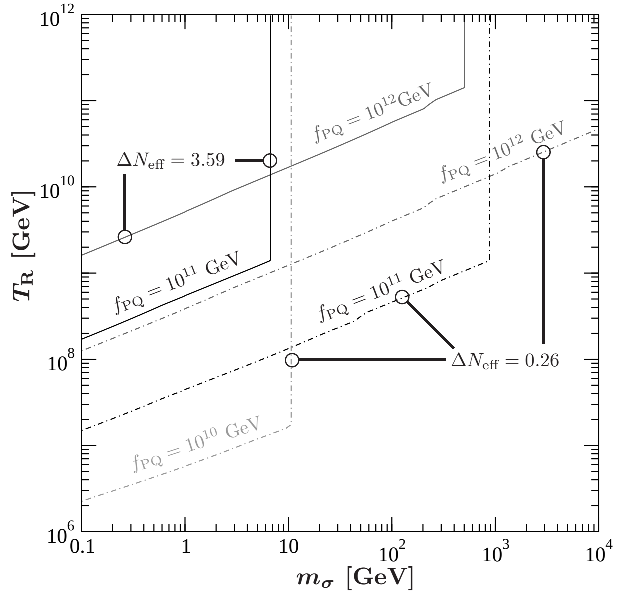

FIG. 6. Contours of ΔN_{eff} at $T \ll 1$ MeV provided by non-thermally produced axions from decays of thermal saxions for $x = 1$ and $f_{\mathrm{PQ}} = 10^{10}$ GeV (light gray), 10^{11} GeV (black), and 10^{12} GeV (gray). The solid lines show the 2σ CMB + HPS + HST constraint $\Delta N_{\mathrm{eff}} < 3.59$ which imposes upper limits on the reheating temperature T_{R}. For $f_{\mathrm{PQ}} = 10^{10}$ GeV, the T_{R} limit appears at smaller m_σ outside of the considered range. The dash-dotted contours indicate the expected Planck sensitivity of $\Delta N_{\mathrm{eff}} = 0.26$.

$\Delta N_{\mathrm{eff}} = 1.73$ and the dash-dotted lines $\Delta N_{\mathrm{eff}} = 0.26$. The latter is the expected 68% CL accuracy of the Planck satellite mission [53, 54] mentioned already in the Introduction. To guide the eye, we show again the $T_\sigma = 1$ and 10 MeV contours as dotted lines. Here we can provide the ΔN_{eff} contours also in the region with $T_\sigma = 1$ MeV. However, as described in the Introduction, additional restrictive constraints are expected in that region.

In comparison to the BBN-imposed limits, one finds that the shown 2σ limit from precision cosmology disfavors basically the same parameter region as the conservative 3σ limit shown in Fig. 4. The results from precision cosmology thereby allow for a slightly larger ΔN_{eff} at given values of m_σ, f_{PQ}, and T_{R}. Indeed, comparing the mean and the 2σ limit in Table II with the posterior maxima and the 3σ limits from the BBN study, one finds a potential hint towards a ΔN_{eff} value at $T \ll 1$ MeV that is higher than the one at $T \sim 1$ MeV. As discussed already in the preceding section, this may be a first hint for $\Delta N_{\mathrm{eff}} \sim 1$ already prior to BBN due to axions from saxion decays plus an additional late contribution from gravitino NLSP decays into axions and LSP axinos such that $\Delta N_{\mathrm{eff}} \sim 2$ at the time of CMB recombination. With the expected ΔN_{eff} sensitivity of the Planck satellite mission, this possibility will be tested further soon. Moreover, for scenarios in which axions from saxion decays are the only significant source for ΔN_{eff}, the Planck results will allow us to probe significant regions of the m_σ–f_{PQ} parameter space which have not been accessible by ΔN_{eff} studies so far. For fixed T_{R} values, this is indicated by the dot-dashed lines in Fig. 5.

The limits shown in Figs. 4 and 5 in the m_σ–f_{PQ} plane for fixed T_{R} values can be translated into upper limits on the reheating temperature T_{R}. In Fig. 6 the solid lines show the upper limits on T_{R} imposed by the 2σ CMB + HPS + HST constraint $\Delta N_{\mathrm{eff}} < 3.59$ as a function of m_σ for $x = 1$ and $f_{\mathrm{PQ}} = 10^{11}$ GeV (black) and 10^{12} GeV (gray). The expected Planck sensitivity $\Delta N_{\mathrm{eff}} = 0.26$ is indicated by the corresponding dash-dotted lines and in light gray for $f_{\mathrm{PQ}} = 10^{10}$ GeV. Note that the upper limit does not show up for the latter f_{PQ} value in the considered m_σ range. The T_{R} dependence of the contours is described by (32) and disappears for cosmological scenarios with $T_{\mathrm{R}} \gtrsim T_{\mathrm{D}}$ where (31) applies. Here we should stress that the shown upper limits on T_{R} rely on non-thermally produced axions from decays of thermal saxions providing the only significant contribution to ΔN_{eff} at $T \ll 1$ MeV. In scenarios with additional sizable contributions (e.g., from late gravitino NLSP decays into an axino LSP and the axion), the considered extra radiation constraint will impose more restrictive T_{R} limits. Nevertheless, the shown upper limits will remain to be applicable as conservative guaranteed limits.

Let us compare our results shown in Fig. 6 with existing results. For example, the yellow curve in Fig. 5(a) of Ref. [11] presents an upper T_{R} limit imposed by

$\Delta N_{\rm eff} \leq 1$ that disfavors basically $T_{\rm R} > 10^6\,$GeV for $f_{\rm PQ} = 10^{10}\,$GeV and the whole m_σ range considered above. With the assumed initial saxion field displacement of $\sigma_{\rm i} \sim f_{\rm PQ}$, that existing limit is governed also by thermal saxions that decay into axions. However, we find that it is overly restrictive due to the omission of the factor $[g_{*S}(T_\sigma)/g_{*S}(T)]^{4/3}$ in Eq. (24) of Ref. [11]. Thereby, our $\Delta N_{\rm eff}$ expression (30) shows different dependences on $g_{*S}(T)$ and $g_{*S}(T_\sigma)$. Remaining differences are due to the result from our explicit calculation of the thermal saxion production rate and the different definitions of the PQ scale addressed already in footnotes 2 and 3 above. As a result, we find that a large part of the (m_σ, $f_{\rm PQ}$, $T_{\rm R}$) region previously thought to be excluded is actually not restricted by the amount of additional radiation from late decays of thermal saxions.

VIII. RELIC AXION DENSITY

We find it instructive to compare the density parameters of three different axion populations that can be present today in the considered SUSY axion models: (i) $\Omega_a^{\rm eq/TP}h^2$ of thermal relic/thermally produced axions, (ii) $\Omega_a^{\rm NTP}h^2$ of non-thermally produced axions from decays of thermal saxions, and (iii) $\Omega_a^{\rm MIS}h^2$ of the axion condensate from the misalignment mechanism. The latter originates from coherent oscillations of the axion field after it acquires a mass due to instanton effects at $T \lesssim 1$ GeV. This is the axion population that can provide the cold dark matter in our Universe, as mentioned at the end of Sect. VII A. For details on this misalignment mechanism we refer to [1, 2, 7] and references therein. Here we quote the density parameter,

$$\Omega_a^{\rm MIS}h^2 \sim 0.15\,\theta_i^2 \left(\frac{f_{\rm PQ}}{10^{12}\,{\rm GeV}}\right)^{\frac{7}{6}}, \qquad (39)$$

which is governed by the initial misalignment angle θ_i of the axion field. This expression applies to non-SUSY and SUSY settings. In the considered case in which the PQ symmetry breaks before inflation and is not restored thereafter, $T_{\rm R} < f_{\rm PQ}$, a single θ_i value will enter (39). Since thermal processes involving axions proceed at negligible rates at $T \lesssim 1$ GeV for $f_{\rm PQ}$ respecting (6), the axion condensate cannot be thermalized. Accordingly, $\Omega_a^{\rm MIS}h^2$ can coexist with $\Omega_a^{\rm eq/TP}h^2$ and $\Omega_a^{\rm NTP}h^2$, which we calculate in the following.

Since thermal relic and thermally produced axions have (basically) a thermal spectrum, one can describe the associated density parameter approximately by

$$\Omega_a^{\rm eq/TP}h^2 \simeq \sqrt{\langle p_{a,0}^{\rm th}\rangle^2 + m_a^2}\; Y_a^{\rm eq/TP}\; s(T_0)h^2/\rho_c, \qquad (40)$$

where $\rho_c/[s(T_0)h^2] = 3.6$ eV and $Y_a^{\rm eq/TP} = Y_\sigma^{\rm eq/TP}$ as described in Sect. V. With the present CMB temperature of $T_0 = 0.235$ meV and an axion temperature today of $T_{a,0} = [g_{*S}(T_0)/228.75]^{1/3}\,T_0 \simeq 0.06$ meV, the average momentum of thermal axions today is given by $\langle p_{a,0}^{\rm th}\rangle = 2.701\,T_{a,0}$. When comparing this momentum with the axion mass m_a, one finds that this axion population is still relativistic today for $f_{\rm PQ} \gtrsim 10^{11}$ GeV. At and before the CMB decoupling epoch, $T \gtrsim 1$ eV, axions from thermal processes were relativistic for $f_{\rm PQ}$ in the full allowed range (6). In the considered SUSY settings, they contribute at most

$$\Delta N_{\rm eff}(T) = \frac{4}{7}\left(\frac{T_a}{T_\nu}\right)^4 = \frac{4}{7}\left[\frac{g_{*S}(T)}{228.75}\right]^{4/3}\left(\frac{T}{T_\nu}\right)^4, \qquad (41)$$

i.e., $\Delta N_{\rm eff}(T) \leq 0.0097$ for 10 MeV $\gtrsim T \gtrsim 1$ eV, which is far below the Planck sensitivity and easily accommodated by the $\Delta N_{\rm eff}$ limits discussed above.

The density parameter of non-thermal axions emitted in late decays of saxions from thermal processes reads

$$\Omega_a^{\rm NTP}h^2 = 2\sqrt{(p_{a,0}^{\rm NTP})^2 + m_a^2}\; Y_\sigma^{\rm eq/TP}\; s(T_0)h^2/\rho_c \qquad (42)$$

with the present momentum of these axions given by

$$p_{a,0}^{\rm NTP} = \frac{m_\sigma}{2}\left[\frac{g_{*S}(T_0)}{g_{*S}(T_\sigma)}\right]^{1/3}\frac{T_0}{T_\sigma}, \qquad (43)$$

when applying the sudden decay approximation. Thus, $\Omega_a^{\rm NTP}h^2$ will depend on m_σ if these axions are still relativistic today, i.e., when $T_0 \gtrsim T_{\rm nr}$ given by (36) above. As extensively discussed in the previous section, this non-thermal axion population can provide a significant contribution to $\Delta N_{\rm eff}$ prior to BBN and thereafter. In fact, one can use (26) to relate $\Omega_a^{\rm NTP}h^2$ to this $\Delta N_{\rm eff}$:

$$\Omega_a^{\rm NTP}h^2 = \left\{1.1\times10^{-11}\left(\frac{10^9\,{\rm GeV}}{f_{\rm PQ}}\right)^2\left(\frac{Y_\sigma^{\rm eq/TP}}{10^{-3}}\right)^2 + 3.2\times10^{-11}\left(\frac{T_\nu}{T}\right)^8\left[\frac{10.75}{g_{*S}(T)}\right]^{8/3}\Delta N_{\rm eff}^2(T)\right\}^{1/2}, \qquad (44)$$

where the m_σ dependence is now absorbed into $\Delta N_{\rm eff}(T)$. Thus, the discussed $\Delta N_{\rm eff}$ constraints translate directly into upper limits on $\Omega_a^{\rm NTP}h^2$. For $T \lesssim 1$ MeV and $f_{\rm PQ}$ such that the first term on the right-hand side of (44) is negligible, those limits are described by $\Omega_a^{\rm NTP}h^2 = 5.7\times10^{-6}\,\Delta N_{\rm eff}$. (This applies to thermal axions as well if they are still relativistic today.)

Figure 7 shows $\Omega_a^{\rm NTP}h^2$ contours that correspond to $\Delta N_{\rm eff}$ values of 3.59 (solid), 1.73 (dashed), and 0.26 (dash-dotted). As in Fig. 5, these values are motivated by the CMB + HPS + HST result [48] quoted in Table II and the expected 68% CL sensitivity of the Planck satellite mission [53, 54]. Contours of $\Omega_a^{\rm eq/TP}h^2$ are shown for $T_{\rm R} = 10^8$ (10^{10}) GeV by the solid black (gray) lines and for larger $T_{\rm R} > T_{\rm D}$ by the unlabeled dotted line. On this dotted line at $f_{\rm PQ} > 10^{11}\,$GeV, (41) applies so that $\Delta N_{\rm eff} = 0.0097$ and $\Omega_a^{\rm eq}h^2 = 5.5\times10^{-8}$ reside in thermal relic axions that are still relativistic today. The

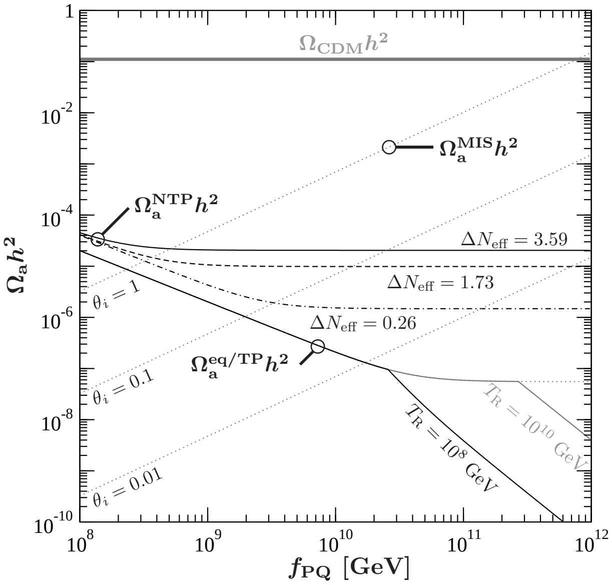

FIG. 7. The density parameters of the axion condensate from the misalignment mechanism $\Omega_a^{\mathrm{MIS}}h^2$ for $\theta_i = 0.01$, 0.1, and 1 (dotted lines), of non-thermally produced axions from decays of thermal saxions $\Omega_a^{\mathrm{NTP}}h^2$ for $\Delta N_{\mathrm{eff}} = 3.59$ (solid), 1.73 (dashed), and 0.26 (dash-dotted), and of thermal relic/thermally produced axions $\Omega_a^{\mathrm{eq/TP}}h^2$ for $T_{\mathrm{R}} = 10^8$ (black) and 10^{10} GeV (gray). The dotted line connected to the latter indicates $\Omega_a^{\mathrm{eq}}h^2$ for larger T_{R} with $T_{\mathrm{R}} > T_{\mathrm{D}}$. The dark matter density parameter $\Omega_{\mathrm{CDM}}h^2 \simeq 0.1$ [60] is indicated by the horizontal gray bar. As in Fig. 5, we consider ΔN_{eff} at $T \ll 1$ and show values based on the CMB + HPS + HST result [48] quoted in Table II and the expected 68% CL sensitivity of the Planck satellite mission [53, 54].

labeled dotted lines indicate $\Omega_a^{\mathrm{MIS}}h^2$ of the axion condensate from the misalignment mechanism for $\theta_i = 0.01$, 0.1, and 1. For $\theta_i \sim 1$ and $f_{\mathrm{PQ}} \sim 10^{12}$ GeV, this cold axion population can explain the dark matter density $\Omega_{\mathrm{CDM}}h^2 \simeq 0.1$ [60] displayed by the gray bar.

Considering the 2σ limit $\Delta N_{\mathrm{eff}} < 3.59$ in Fig. 7, one sees that it constrains $\Omega_a^{\mathrm{NTP}}h^2$ to values that stay below the photon density $\Omega_\gamma h^2 \simeq 2.5 \times 10^{-5}$ [60]. Remarkably, Planck results are expected to probe even much smaller Ω_a^{NTP}. The testable values can be as small as an order of magnitude below Ω_γ if axions emitted in decays of thermal saxions are the only significant contribution to ΔN_{eff}. In contrast and similarly to the non-SUSY case [17], it will remain to be extremely challenging to probe the axion population from thermal processes with its small contribution of $\Delta N_{\mathrm{eff}} \lesssim 0.01$.

Note that m_σ changes along the $\Omega_a^{\mathrm{NTP}}h^2$ curves in Fig. 7 for fixed T_{R} and x since we indicate results for fixed values of ΔN_{eff}. Indeed, additional BBN constraints can disfavor parts of the shown contours when $T_\sigma < 1$ MeV. For $T_\sigma > 1$ MeV, BBN constraints on ΔN_{eff} – such as the ones considered in Fig. 4 – can also be displayed in terms of $\Omega_a^{\mathrm{NTP}}h^2$. On the logarithmic scale considered in Fig. 7, they are similar to the shown ones.

Taking into account the relation between f_{PQ} and m_a, the analog of a Lee–Weinberg curve is given by $\Omega_a h^2 \geq \Omega_a^{\mathrm{MIS}}h^2 + \Omega_a^{\mathrm{NTP}}h^2 + \Omega_a^{\mathrm{eq/TP}}h^2$ and can be inferred from Fig. 7. Depending on the initial displacement of the saxion field from the vacuum, σ_i, and on the mass spectrum, there can be additional contributions to the axion density parameter, e.g., from decays of the saxion condensate into axions and/or a gravitino NLSP into axions and LSP axinos. In such cases, sizable additional contributions also to ΔN_{eff} are possible which will affect the $\Omega_a^{\mathrm{NTP}}h^2$ contours in Fig. 7. Thus the shown contours should be understood as conservative maximum values.

One can consider Fig. 7 as a SUSY generalization of Fig. 4 in Ref. [17], which allows one to infer the axion analog of the Lee–Weinberg curve in non-SUSY scenarios. Whereas $\Omega_a^{\mathrm{eq/TP}}h^2$ can govern the axion density for small θ_i and/or small f_{PQ} in non-SUSY scenarios [17], we find $\Omega_a^{\mathrm{NTP}}h^2 \gtrsim 2\,\Omega_a^{\mathrm{eq/TP}}h^2$ in the considered SUSY scenarios. This can be seen in Fig. 7 and when comparing (40) and (42). If SUSY and a hadronic axion model are realized in nature, the axion density parameter can thus be governed by non-thermal axions from decays of thermal saxions and/or the axion condensate from the misalignment mechanism. Interestingly, both of these populations may be accessible experimentally: While signals of the axion condensate are expected in direct axion dark matter searches [80], the findings of ΔN_{eff} studies may already be first hints for the existence of non-thermal axions from saxion decays.

IX. CONCLUSION

We have explored thermal production processes of axions and saxions in the primordial plasma, resulting axion populations and their manifestations in the form of extra radiation ΔN_{eff} prior to BBN and well thereafter. The considered SUSY axion models are attractive for a number of reasons. For example, they allow for simultaneous solutions of the strong CP problem, the hierarchy problem, and the dark matter problem.

Here we have focussed on the saxion, which can be a late decaying particle and as such be subject to various cosmological constraints. We find that the saxion decay into two axions is often the dominating one. For a saxion mass of $m_\sigma \gtrsim 1$ GeV, such decays occur typically before the onset of BBN. We have shown that the emitted axions can then still be relativistic at the large scattering surface. Thereby, they can provide sizable contributions to extra radiation ΔN_{eff} that is testable in BBN studies and in precision cosmology of the CMB and the LSS.

We have aimed at a consistent description of both the thermal axion/saxion production and of saxion decays into axions. This has motivated our careful derivations of the Lagrangian $\mathcal{L}_{\mathrm{PQ}}^{\mathrm{int}}$ that describes the interactions of the PQ multiplet with quarks, gluons, squarks, and gluinos and of $\mathcal{L}_{\mathrm{PQ}}^{\mathrm{kin}}$ that describes the interactions of saxions with axions in addition to their kinetic terms. The requirement of canonically normalized kinetic terms defines the scale $v_{\rm PQ}$, which governs the saxion-axion-interaction strength together with another PQ-model-dependent parameter $x \lesssim 1$. On the other hand, the form of the effective axion-gluon-interaction term defines the PQ scale $f_{\rm PQ}$. Considering the emergence of this term from loops of heavy KSVZ fields in an explicit hadronic axion model, we find $f_{\rm PQ} = \sqrt{2} v_{\rm PQ}$. This is in contrast to numerous existing studies which treat $v_{\rm PQ}$ and $f_{\rm PQ}$ synonymously.

Relying on the derived form of $\mathcal{L}_{\rm PQ}^{\rm int}$, we have calculated the thermal production rates of saxions and axions and the resulting yields in the hot early Universe. Despite differences in the interaction terms, we find that the rate for thermal saxion production agrees with the one for thermal axion production. This implies an agreement also of the calculated thermally produced yields and of our estimates of the decoupling temperatures $T_{\rm D}$. By applying HTL resummation [30] and the Braaten–Yuan prescription [31], finite results are obtained in a gauge-invariant way consistent to leading order in the coupling constant and screening effects are treated systematically.

Using our result for the thermally produced saxion yield, we have calculated $\Delta N_{\rm eff}$ provided in the form of axions from decays of thermal saxions. This has allowed us to demonstrate that such a $\Delta N_{\rm eff}$ contribution can indeed explain the trends towards extra radiation beyond the SM seen in recent studies of BBN, CMB, and LSS.

To account for the current PDG recommendation for the free neutron lifetime, $\tau_{\rm n} = 880.1 \pm 1.1$ s [60], we have performed a BBN likelihood analysis with `PArthENoPE` [68] and based on recent insights on the primordial abundances of ^{4}He [46, 47] and D [66]. For $\Delta N_{\rm eff}$ at the onset of BBN, we thereby obtain posterior maxima of 0.76 and 0.77 and 3σ upper limits of 1.97 and 3.53 with the $Y_{\rm p}$ results of [46] and [47], respectively. When comparing these values with results from studies of the CMB and LSS, we find that the latter provide compatible but more pronounced hints for extra radiation. For example, the precision cosmology study of [48] reports a mean of 1.73 and a 2σ limit 3.59 for $\Delta N_{\rm eff}$ at $T \ll 1$ MeV when using the CMB + HPS + HST data set.

We have translated the upper limits on $\Delta N_{\rm eff}$ quoted above into bounds on $f_{\rm PQ}$, m_σ, and $T_{\rm R}$. These bounds can disfavor significant regions of the m_σ–$f_{\rm PQ}$ parameter plane in high $T_{\rm R}$ scenarios. However, we find that our limits leave open a considerable parameter region previously thought to be excluded [11]. Significant parts of the allowed parameter region have been identified, which will become accessible very soon with the upcoming results from the Planck satellite mission.

The explanation of the above hints for extra radiation via axions from decays of thermal saxions requires a relatively high reheating temperature of $T_{\rm R} \gtrsim 10^7$ GeV for $m_\sigma \gtrsim 0.1$ GeV. Such high $T_{\rm R}$ scenarios can be in conflict with cosmological constraints due to overly efficient thermal production of axinos and gravitinos. To illustrate the viability of $\Delta N_{\rm eff} \sim 1$ from saxion decays, we have described two exemplary SUSY scenarios which allow for $T_{\rm R} = 10^8$ and 10^{10} GeV:

(i) With the gravitino LSP as cold dark matter and a sneutrino NLSP, the presented $\Delta N_{\rm eff} \sim 1$ explanation for $T_{\rm R} = 10^8$ GeV can be viable for $m_\sigma \sim m_{3/2} \sim 10$ GeV and $m_{\tilde{g}} \sim 1$ TeV. This explanation requires $f_{\rm PQ} \sim 10^{10}$ GeV and heavy axinos, $m_{\tilde{a}} \gtrsim 2$ TeV, which decay prior to NLSP decoupling. Here $\Delta N_{\rm eff} \sim 1$ is already present at the onset of BBN and does not change thereafter. Accordingly, we expect that the Planck results will point to a $\Delta N_{\rm eff}$ value that is consistent with the one inferred from BBN studies.

(ii) With a very light axino LSP, $m_{\tilde{a}} \lesssim 37$ eV, as hot dark matter and a gravitino NLSP, the $\Delta N_{\rm eff} \sim 1$ explanation for $T_{\rm R} = 10^{10}$ GeV can be viable for $m_\sigma \sim m_{3/2} \sim 100$ GeV and $m_{\tilde{g}} \sim 1$ TeV. Here this explanation requires $f_{\rm PQ} \sim 10^{12}$ GeV so that cold dark matter can be provided by the axion misalignment mechanism. With the stau as the LOSP, further potential BBN constraints can be evaded. Note that $T_{\rm R} = 10^{10}$ GeV allows for successful thermal leptogenesis. The saxion decays give $\Delta N_{\rm eff} \sim 1$ already at the onset of BBN. However, late gravitino NLSP decays into the axion and the axino LSP can provide an additional contribution of $\Delta N_{\rm eff} \sim 1$ well after BBN [61, 78]. Thus, it will be interesting to see whether the Planck results confirm the trend towards an excess of extra radiation that is more pronounced at late times. For example, the finding of $\Delta N_{\rm eff} \sim 2$ at late times will be a possible signature expected in this setting.

If a SUSY hadronic axion model is realized in nature, three different axion populations will be present today: thermally produced/thermal relic axions, non-thermally produced axions from decays of thermal saxions, and the axion condensate from the misalignment mechanism. We have calculated and compared the associated density parameters. The results allow us to infer the axion analog of the Lee–Weinberg curve. For $f_{\rm PQ} \gtrsim 10^{12}$ GeV and an initial misalignment angle of $\theta_i \sim 1$, the axion density parameter is governed by the axion condensate. In that parameter region this population may be accessible in direct axion dark matter searches. For smaller $f_{\rm PQ}$ and smaller θ_i, axions from saxion decays can dominate the axion density parameter. While it will be extremely challenging to probe thermal axions, Planck may confirm $\Delta N_{\rm eff}$ signals of this non-thermally produced population in the full allowed $f_{\rm PQ}$ range. Since the considered axion populations can coexist, there is the exciting chance to see signals of both axion dark matter and axion dark radiation in current and future experiments.

ACKNOWLEDGMENTS

We are grateful to S. Halter, G. Raffelt, S. Sarikas, and Y.Y.Y. Wong for valuable discussions. This research was partially supported by the Cluster of Excellence "Origin and Structure of the Universe."

---

[1] P. Sikivie, Lect. Notes Phys. **741**, 19 (2008), arXiv:astro-ph/0610440.

[2] J. E. Kim and G. Carosi, Rev.Mod.Phys. **82**, 557 (2010), arXiv:0807.3125.

[3] S. P. Martin, A Supersymmetry Primer, (1997), arXiv:hep-ph/9709356.

[4] M. Drees, R. Godbole, and P. Roy, Theory and phenomenology of sparticles, (2004), Hackensack, USA: World Scientific 555p.

[5] H. Baer and X. Tata, Weak scale supersymmetry, (2006), Cambridge, UK: Univ. Pr. 537 p.

[6] H. K. Dreiner, H. E. Haber, and S. P. Martin, Phys.Rept. **494**, 1 (2010), arXiv:0812.1594.

[7] M. Beltran, J. Garcia-Bellido, and J. Lesgourgues, Phys. Rev. **D75**, 103507 (2007), arXiv:hep-ph/0606107.

[8] S. Chang and H. B. Kim, Phys.Rev.Lett. **77**, 591 (1996), arXiv:hep-ph/9604222.

[9] M. Hashimoto, K. I. Izawa, M. Yamaguchi, and T. Yanagida, Phys. Lett. **B437**, 44 (1998), arXiv:hep-ph/9803263.

[10] T. Asaka and M. Yamaguchi, Phys. Lett. **B437**, 51 (1998), arXiv:hep-ph/9805449.

[11] M. Kawasaki, K. Nakayama, and M. Senami, JCAP **0803**, 009 (2008), arXiv:0711.3083.

[12] M. Kawasaki, N. Kitajima, and K. Nakayama, (2011), arXiv:1112.2818.

[13] M. S. Turner, Phys. Rev. Lett. **59**, 2489 (1987).

[14] S. Chang and K. Choi, Phys. Lett. **B316**, 51 (1993), arXiv:hep-ph/9306216.

[15] E. Masso, F. Rota, and G. Zsembinszki, Phys. Rev. **D66**, 023004 (2002), arXiv:hep-ph/0203221.

[16] S. Hannestad, A. Mirizzi, and G. Raffelt, JCAP **0507**, 002 (2005), arXiv:hep-ph/0504059.

[17] P. Graf and F. D. Steffen, Phys. Rev. **D83**, 075011 (2011), arXiv:1008.4528.

[18] J. E. Kim, Phys. Rev. Lett. **67**, 3465 (1991).

[19] K. Rajagopal, M. S. Turner, and F. Wilczek, Nucl. Phys. **B358**, 447 (1991).

[20] S. A. Bonometto, F. Gabbiani, and A. Masiero, Phys. Rev. **D49**, 3918 (1994), arXiv:hep-ph/9305237.

[21] E. J. Chun and A. Lukas, Phys. Lett. **B357**, 43 (1995), arXiv:hep-ph/9503233.

[22] T. Asaka and T. Yanagida, Phys.Lett. **B494**, 297 (2000), arXiv:hep-ph/0006211.

[23] L. Covi, H.-B. Kim, J. E. Kim, and L. Roszkowski, JHEP **05**, 033 (2001), arXiv:hep-ph/0101009.

[24] A. Brandenburg and F. D. Steffen, JCAP **0408**, 008 (2004), arXiv:hep-ph/0405158.

[25] A. Strumia, JHEP **06**, 036 (2010), arXiv:1003.5847.

[26] E. J. Chun, Phys.Rev. **D84**, 043509 (2011), arXiv:1104.2219.

[27] K. J. Bae, K. Choi, and S. H. Im, JHEP **1108**, 065 (2011), arXiv:1106.2452.

[28] K.-Y. Choi, L. Covi, J. E. Kim, and L. Roszkowski, JHEP **1204**, 106 (2012), arXiv:1108.2282.

[29] K. J. Bae, E. J. Chun, and S. H. Im, JCAP **1203**, 013 (2012), arXiv:1111.5962.

[30] E. Braaten and R. D. Pisarski, Nucl. Phys. **B337**, 569 (1990).

[31] E. Braaten and T. C. Yuan, Phys. Rev. Lett. **66**, 2183 (1991).

[32] M. Bolz, A. Brandenburg, and W. Buchmüller, Nucl. Phys. **B606**, 518 (2001), arXiv:hep-ph/0012052.

[33] J. Pradler and F. D. Steffen, Phys. Rev. **D75**, 023509 (2007), arXiv:hep-ph/0608344.

[34] J. Pradler and F. D. Steffen, Phys. Lett. **B648**, 224 (2007), arXiv:hep-ph/0612291.

[35] J. Pradler, Electroweak Contributions to Thermal Gravitino Production, Diploma thesis, Univ. of Vienna, 2006.

[36] P. Graf, Axions in the Early Universe, Diploma thesis, Univ. of Regensburg, 2009.

[37] F. D. Steffen, Eur. Phys. J. **C59**, 557 (2009), arXiv:0811.3347.

[38] L. Covi and J. E. Kim, New J. Phys. **11**, 105003 (2009), arXiv:0902.0769.

[39] T. Asaka and M. Yamaguchi, Phys. Rev. **D59**, 125003 (1999), arXiv:hep-ph/9811451.

[40] M. Kawasaki and T. Yanagida, Phys. Lett. **B399**, 45 (1997), arXiv:hep-ph/9701346.

[41] X.-L. Chen and M. Kamionkowski, Phys. Rev. **D70**, 043502 (2004), arXiv:astro-ph/0310473.

[42] D. H. Lyth, Phys. Rev. **D48**, 4523 (1993), arXiv:hep-ph/9306293.

[43] J. Hasenkamp and J. Kersten, Phys. Rev. **D82**, 115029 (2010), arXiv:1008.1740.

[44] H. Baer, S. Kraml, A. Lessa, and S. Sekmen, JCAP **1104**, 039 (2011), arXiv:1012.3769.

[45] K. Choi, E. J. Chun, and J. E. Kim, Phys. Lett. **B403**, 209 (1997), arXiv:hep-ph/9608222.

[46] Y. I. Izotov and T. X. Thuan, Astrophys. J. **710**, L67 (2010), arXiv:1001.4440.

[47] E. Aver, K. A. Olive, and E. D. Skillman, JCAP **1005**, 003 (2010), arXiv:1001.5218.

[48] J. Hamann, S. Hannestad, J. Lesgourgues, C. Rampf, and Y. Y. Y. Wong, JCAP **1007**, 022 (2010), arXiv:1003.3999.

[49] J. Hamann, S. Hannestad, G. G. Raffelt, and Y. Y. Y. Wong, JCAP **0708**, 021 (2007), arXiv:0705.0440.

[50] B. A. Reid, L. Verde, R. Jimenez, and O. Mena, JCAP **1001**, 003 (2010), arXiv:0910.0008.

[51] WMAP, E. Komatsu *et al.*, Astrophys. J. Suppl. **192**, 18 (2011), arXiv:1001.4538.

[52] M. C. Gonzalez-Garcia, M. Maltoni, and J. Salvado, JHEP **08**, 117 (2010), arXiv:1006.3795.

[53] L. Perotto, J. Lesgourgues, S. Hannestad, H. Tu, and Y. Y. Y. Wong, JCAP **0610**, 013 (2006), arXiv:astro-ph/0606227.

[54] J. Hamann, J. Lesgourgues, and G. Mangano, JCAP **0803**, 004 (2008), arXiv:0712.2826.

[55] T. Kugo, I. Ojima, and T. Yanagida, Phys. Lett. **B135**, 402 (1984).

[56] J. E. Kim, Phys. Rev. Lett. **43**, 103 (1979).

[57] M. A. Shifman, A. I. Vainshtein, and V. I. Zakharov, Nucl. Phys. **B166**, 493 (1980).

[58] M. Kawasaki, N. Kitajima, and K. Nakayama, Phys.Rev. **D83**, 123521 (2011), arXiv:1104.1262.

[59] G. G. Raffelt, Lect. Notes Phys. **741**, 51 (2008), arXiv:hep-ph/0611350.

[60] Particle Data Group, J. Beringer *et al.*, Phys. Rev. **D86**, 010001 (2012).

[61] K. Ichikawa, M. Kawasaki, K. Nakayama, M. Senami, and F. Takahashi, JCAP **0705**, 008 (2007),

arXiv:hep-ph/0703034.

[62] T. Moroi and M. Takimoto, (2012), arXiv:1207.4858.

[63] T. Hahn, Comput. Phys. Commun. **140**, 418 (2001), arXiv:hep-ph/0012260.

[64] T. Hahn and M. Perez-Victoria, Comput. Phys. Commun. **118**, 153 (1999), arXiv:hep-ph/9807565.

[65] G. Mangano *et al.*, Nucl. Phys. **B729**, 221 (2005), arXiv:hep-ph/0506164.

[66] M. Pettini, B. J. Zych, M. T. Murphy, A. Lewis, and C. C. Steidel, Monthly Notices of the Royal Astronomical Society **391**, 1499 (2008).

[67] J. Hamann, S. Hannestad, G. G. Raffelt, and Y. Y. Wong, JCAP **1109**, 034 (2011), arXiv:1108.4136.

[68] O. Pisanti *et al.*, Comp. Phys. Commun. **178**, 956 (2008), arXiv:0705.0290.

[69] Particle Data Group, K. Nakamura *et al.*, J. Phys. **G37**, 075021 (2010).

[70] J. Hamann, S. Hannestad, G. G. Raffelt, I. Tamborra, and Y. Y. Wong, Phys.Rev.Lett. **105**, 181301 (2010), arXiv:1006.5276.

[71] J. L. Feng, S. Su, and F. Takayama, Phys.Rev. **D70**, 075019 (2004), arXiv:hep-ph/0404231.

[72] T. Kanzaki, M. Kawasaki, K. Kohri, and T. Moroi, Phys.Rev. **D75**, 025011 (2007), arXiv:hep-ph/0609246.

[73] J. R. Ellis, K. A. Olive, and Y. Santoso, JHEP **0810**, 005 (2008), arXiv:0807.3736.

[74] A. Freitas, F. D. Steffen, N. Tajuddin, and D. Wyler, Phys.Lett. **B679**, 270 (2009), arXiv:0904.3218.

[75] A. Freitas, F. D. Steffen, N. Tajuddin, and D. Wyler, Phys.Lett. **B682**, 193 (2009), arXiv:0909.3293.

[76] A. Freitas, F. D. Steffen, N. Tajuddin, and D. Wyler, JHEP **1106**, 036 (2011), arXiv:1105.1113.

[77] K. A. Olive, D. N. Schramm, and M. Srednicki, Nucl.Phys. **B255**, 495 (1985).

[78] J. Hasenkamp, Phys.Lett. **B707**, 121 (2012), arXiv:1107.4319.

[79] W. Buchmüller, R. Peccei, and T. Yanagida, Ann.Rev.Nucl.Part.Sci. **55**, 311 (2005), arXiv:hep-ph/0502169.

[80] G. Carosi and K. van Bibber, Lect.Notes Phys. **741**, 135 (2008), arXiv:hep-ex/0701025.